Energy Advances

Accepted Manuscript

This article can be cited before page numbers have been issued, to do this please use: T. F. Santos, C. M. Santos, V. V. Kumar , B. S. Nzeyimana, H. Jeevan Rao, B. Akkinepally, D. F. de Santana Souza and J. H. O. D. Nascimento, *Energy Adv.*, 2026, DOI: 10.1039/D5YA00363F.

View Article Online
DOI: 10.1039/D5YA00363F

REVIEW

Received 30th July 2025,

Accepted 00th January 20xx

DOI: 10.1039/x0xx00000x

Flexible Perovskite Solar Cells: Materials Design, Environmental Stability, and Sustainable Strategies for All-Environment Photovoltaics

Thiago F. Santos[a,b*] *(Corresponding Author)*, Caroliny M. Santos[a,b], Vishnu Vijay Kumar[c], Bahati Shabani Nzeyimana[d], H Jeevan Rao[e], Bhargav Akkinepally[f], Domingos F. S. Souza[a], and J. H. O. Nascimento[a,b*] *(Corresponding Author)*

Flexible perovskite solar cells (f-PeSCs) are revolutionizing photovoltaic technology with their high efficiency, mechanical adaptability, and potential for cost-effective manufacturing, poised to transform both indoor and outdoor energy markets. This systematic review examines the scientific and technological advancements of f-PeSCs from 2012 to 2024, employing bibliometric analysis and science mapping to identify global trends, collaborative networks, and research gaps. Achieving power conversion efficiencies of 41% under indoor lighting, f-PeSCs are driving a burgeoning market, projected to grow from USD 0.35 billion in 2023 to USD 8.81 billion by 2034, complementing the broader solar cell market expansion from USD 149.45 billion to USD 730.74 billion over the same period. Key innovations include low-temperature deposition, flexible substrates (e.g., PET, PEN, PI), and advanced electrodes, such as carbon-based and metallic nanostructures. Despite progress, challenges persist in scalability, long-term stability, and sustainability of lead-based perovskite. Strategies such as roll-to-roll manufacturing, lead-free formulations, and AI-driven material optimization are crucial for commercialization. Aligned with Sustainable Development Goals (SDGs) such as affordable clean energy (SDG 7), industrial innovation (SDG 9), and climate action (SDG 13), f-PeSCs provide a transformative platform for sustainable energy, supporting the global transition to a low-carbon future.

1. Introduction

Global energy demand has continued to increase steadily over the past decades due to population growth, urbanization, and the expansion of digital infrastructures. According to the International Energy Agency (IEA), global electricity demand is projected to grow by more than 3% annually, with renewable sources playing a critical role in meeting this demand [1]. Photovoltaic technologies currently account for a rapidly expanding share of global electricity generation, with installed PV capacity exceeding 1.6 TW in 2023 [2]. While crystalline silicon solar cells dominate the market with efficiencies exceeding 26% and mature manufacturing infrastructure, they remain limited by rigidity, weight, and high-temperature processing requirements [3,4]. Emerging photovoltaic technologies such as perovskite solar cells offer significant advantages including tunable bandgaps, low-temperature fabrication, and compatibility with flexible substrates. These features position flexible perovskite solar cells as promising candidates for next-generation photovoltaic applications beyond conventional rigid modules. Flexible perovskite solar cells (f-PeSCs) have emerged as a promising technology for next-generation photovoltaic systems, offering a unique combination of high efficiency, mechanical flexibility, and the potential for low-cost, large-scale manufacturing [5,6]. Unlike traditional rigid solar cells, f-PeSCs are lightweight, conformable to curved surfaces, and compatible with roll-to-roll (R2R) manufacturing processes, making them ideal for both indoor and outdoor applications, including wearable electronics, the Internet of Things (IoT), building integration (BIPV), and aerospace systems [7]. Since 2012, the power conversion efficiency (PCE) of f-PeSCs has improved significantly, reaching an impressive 41% under indoor

a. Postgraduate Program in Chemical Engineering, Technology Center, Federal University of Rio Grande do Norte, Natal, Rio Grande do Norte, 59072-970, Brazil.
b. GPIMN - Micro and Nanotechnologies Innovation Research Group, Federal University of Rio Grande do Norte, Natal, Rio Grande do Norte, Brazil
c. Structural Engineering, Division of Engineering, New York University Abu Dhabi (NYUAD), PO Box 129188, Abu Dhabi, United Arab Emirates
d. PG&Research Department of Environmental Science, Bishop Heber College (Autonomous) Affiliated to Bhrathidasan University, Tiruchirappalli, India, 620017
e. Department of Mathematics, School of Sciences and Humanities, Nazarbayev University, Astana 010000, Kazakhstan.
f. School of Mechanical Engineering, Yeungnam University, Daehak-ro, Gyeongsan-si, Gyeongbuk-do 38541, South Korea

---

g. † Footnotes relating to the title and/or authors should appear here.
h. Supplementary Information available: [details of any supplementary information available should be included here]. See DOI: 10.1039/x0xx00000x

View Article Online
DOI: 10.1039/D5YA00363F

lighting conditions in 2024, while rigid perovskite cells (r-PeSCs) reached 26.7% in the same period. These advances reflect innovations in materials such as flexible substrates (PET, PEN, PI), transparent electrodes (conductive oxides, carbon nanomaterials) and low-temperature deposition techniques [8,9]. Despite progress, challenges such as environmental and mechanical stability, scalability, and sustainability remain crucial for commercialization [10,11]. This systematic review analyzes the scientific landscape of f-PeSCs between 2012 and 2024, using bibliometric data and scientific mapping to identify trends, global collaborations, and research gaps. Furthermore, it explores the impact of f-PeSCs on the Sustainable Development Goals (SDGs), highlighting their potential to promote affordable and clean energy (SDG 7), industrial innovation (SDG 9), sustainable cities (SDG 11), responsible production (SDG 12), climate action (SDG 13) and global partnerships (SDG 17). By integrating technical advances, market analyses, and strategies to overcome barriers, this study offers a holistic view of the state of the art and a roadmap for the future of f-PeSCs in the global energy transition.

State of the art overview

Research on f-PeSCs has advanced significantly, consolidating a comprehensive overview of the state of the art as shown in **Table 1**. This review article integrates and expands previous contributions, offering a multidimensional analysis with bibliometric data (2012-2024) and science mapping, such as keyword analysis and thematic clusters, to map global trends and collaborations. In 2017, Djurišić, A. B., et al. [12] laid a solid foundation, discussing materials, architectures, and critical challenges. In 2020, Venkateswararao, Addanki, et al. [13] addressed innovative solutions for indoor design, while Hou, Xueyan, et al. [14] highlighted the potential in f-PeSCs for IoT, focusing on efficiency and stability. From 2021-2023, Wang, Kai-Li, et al. [15], Polyzoidis, Christos, Konstantinos Rogdakis, and Emmanuel Kymakis [16], Barthwal, Swapnil, Rahul Kumar, and Sandeep Pathak [17], Zhu, Xinyi, et al. [18], and highlighted IoT applications and commercialization hurdles such as stability. This study advances by exploring bandgap tuning and tandem designs for artificial lighting, connecting applications to SDGs such as SDG 7 and SDG 11. In 2024, Zhang, Lixiu, et al. [19], Qamar, Muhammad Zain, et al. [20], Kang, Seok Beom, et al. [21], and Kumari, Priti, Seelam Prasanthkumar, and Lingamallu Giribabu [22], addressed stability, flexible electrodes, and interface engineering. This paper complements these analyses by proposing R2R manufacturing, encapsulation techniques, lead-free perovskites, and LCA aligned with SDG 12. Using VOSviewer, it highlights carbon-based electrodes, metallic nanostructures, and collaborations between China, the US, and South Korea. Unlike previous reviews, which focused on specific topics, this study offers a holistic view, integrating technical advances, socio-environmental impacts via SDGs, AI-driven material design, and applications. Its bibliometric analyses reveal the evolution of the field, positioning it as a reference for researchers and industry in the global energy transition.

Table 1. Most cited review articles of f-PeSCs for indoor & outdoor applications.

Article title (year)	Journal	Citations	Key Objective	Ref.
Perovskite solar cells - An overview of critical issues (2017)	Progress in Quantum Electronics	150	Overview PeSCs materials, device architectures, and issues.	[12]
Device characteristics and material developments of indoor photovoltaic devices (2020)	Materials Science and Engineering R: Reports	126	Generate innovative solutions to overcome design challenges.	[13]
Perovskite indoor photovoltaics: opportunity and challenges (2021)	Chemical Science	98	Analyzes the Indoor PV market, trends, challenges, and perovskite potential.	[15]
Indoor application of emerging photovoltaics - Progress, challenges and perspectives (2020)	Journal of Materials Chemistry A	83	Advances in indoor photovoltaics face stability and toxicity hurdles before commercialization	[14]
Indoor Perovskite Photovoltaics for the Internet of Things-Challenges and Opportunities toward Market Uptake (2021)	Advanced Energy Materials	77	Indoor Perovskite PV progress faces IoT integration challenges requiring multidimensional engineering solutions.	[16]
Present Status and Future Perspective of Antimony Chalcogenide (Sb_2X_3) Photovoltaics (2022)	ACS Applied Energy Materials	41	Sb_2X_3 solar cells offer stable, eco-friendly, cost-effective PV solutions.	[17]

View Article Online
DOI: 10.1039/D5YA00363F

The issues on the commercialization of perovskite solar cells (2024)	Materials Futures	24	PeSCs advance but face commercialization hurdles requiring solutions.	19
Perspectives for the conversion of perovskite indoor photovoltaics into IoT reality (2023)	Nanoscale	15	Perovskite Indoor PVs need bandgap tuning, defect control, and engineering strategies.	18
Advancement in indoor energy harvesting through flexible perovskite photovoltaics for self-powered IoT applications (2024)	Nano Energy	7	Flexible perovskite PV for indoor IoT: efficiency, eco-friendly, stable, commercializable.	20
Study of interface engineering on perovskite-based indoor photovoltaics for powering Internet-of-Things (2024)	Chemical Engineering Journal	0	Interface engineering in perovskite indoor PVs to enhance efficiency and stability for IoT devices.	21
Recent progress on perovskite based indoor photovoltaics: Challenges and commercialization (2024)	Solar Energy	0	Advancements, challenges, and commercialization of perovskite-based indoor PVs for IoT applications.	22

2. Methodological framework

The methodology for analyzing f-PeSCs involved systematic steps with data from Scopus, selected for its coverage in materials sciences and energy [23–25]. The search used the string (“flexible”) AND (“perovskite”) in TITLE-ABS-KEY, restricted to articles in English from 1972 to 2024. Of 4,241 initial articles, 3,080 were selected after excluding 1,161 by language, period, or document type criteria as shown in **Figure 1**. Bibliometrics, VOSviewer, and Science Mapping were used to analyze publications, citations, impact, efficiency, stability, indoor/outdoor applications, collaborations, and trends such as wearable IoT, BIPV, and lead-free perovskites. The approach revealed gaps, advances, and future directions.

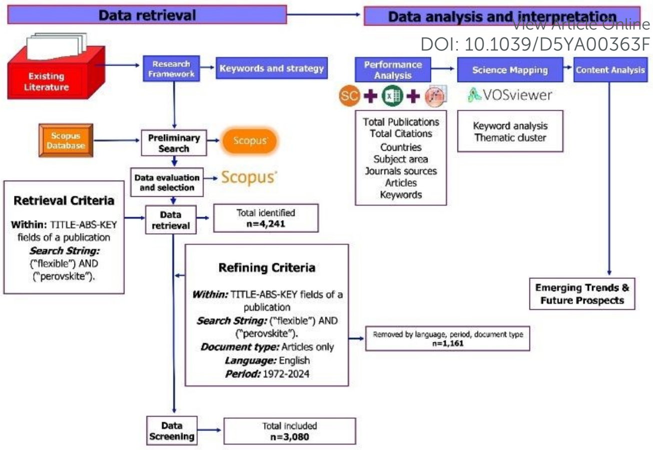

Figure 1. Toolbox for Data Retrieval and Analysis of f-PeSCs in this study

3. Evolution of Flexible Perovskite Solar Cells

The trajectory of f-PeSCs between 2013 and 2024 reveals significant advances in PCE, mechanical and environmental stability, in addition to the diversification of architectures and materials, with important implications for applications in indoor and outdoor environments. In 2013 and 2014, the first implementations of $MAPbI_3$ in regular planar (n-i-p) and inverted planar (p-i-n) architectures as illustrated in **Figure 2**, established the viability of perovskites in flexible structures, validating the potential of organic-inorganic hybrid materials, although with modest PCE below 3% and limited stability [26,27]. In 2015, the use of PET substrates allowed the first functional f-PeSCs, reaching a PCE of 2.62%, which evolved to 7% in the same year, highlighting the importance of flexible substrates compatible with low-temperature processing [28]. Between 2016 and 2017, the introduction of PEN as a substrate resulted in a PCE of 14.85%, while the incorporation of Zn_2SnO_4 as an electron transport layer (ETL) improved mechanical stability, maintaining more than 95% after 300 bending cycles. During this period, mixed compositions such as $(MAPbI_3)_{0.85}(MAPbBr_3)_{0.15}$ were optimized for bandgap tuning and anti-reflection properties, achieving transparency greater than 88% [29,30]. Between 2018 and 2019, the use of C60 electrodes on PEN substrates increased the PCE to 16.8%, combined with transparency greater than 97% and mechanical stability greater than 90% after 1000 cycles. The adoption of additives such as dimethyl sulfide in PET allowed a PCE of 18.4%, even after 5000 bending cycles, evidencing progress in durability [31,32]. From 2020 to 2021, the integration of SnO_2 as ETL achieved a PCE of 19.51%, and the use of PEDOT:EVA as

View Article Online
DOI: 10.1039/D5YA00363F

an encapsulant in PET resulted in a PCE of 19.87%, with environmental stability over 90% after 1000 hours in air and mechanical stability over 95% after 6000 cycles, demonstrating synergy between interface engineering and flexible substrates [33,34]. In 2022, innovative compositions such as $Cs_{0.05}(FA_{0.83}MA_{0.17})_{0.95}Pb(I_{0.83}Br_{0.17})_3$ in PEN achieved PCE of 21.73%, with exceptional stability of 96.78% after 1000 h in 25–35% humidity, while nanocrystalline NiO films in PET achieved PCE of 24.7% for indoor devices in 40–70% humidity, showing adaptability to variable conditions [35]. In 2023, a jump to 32.5% PCE under 1000 lx indoor illumination, using TBAB as an interface modifier in PET, demonstrated potential for IoT and wearable electronics, maintaining more than 80% mechanical stability after 1000 cycles [36]. In 2024, the record PCE of 41% under 1000 lx, with SnO_2/SZC films in PET, combined with environmental stability above 91% after 1200 hours and mechanical stability above 80% after 8000 cycles, positions f-PeSCs as leaders in indoor photovoltaics and BIPV applications [37]. The evolution of f-PeSCs, from the first planar and inverted architectures to the current efficiency records, reflects the maturity of the field, integrating historical data, quantitative analysis, and strategies aligned with the Sustainable Development Goals, offering a roadmap for the next decade of innovation in flexible renewable energy.

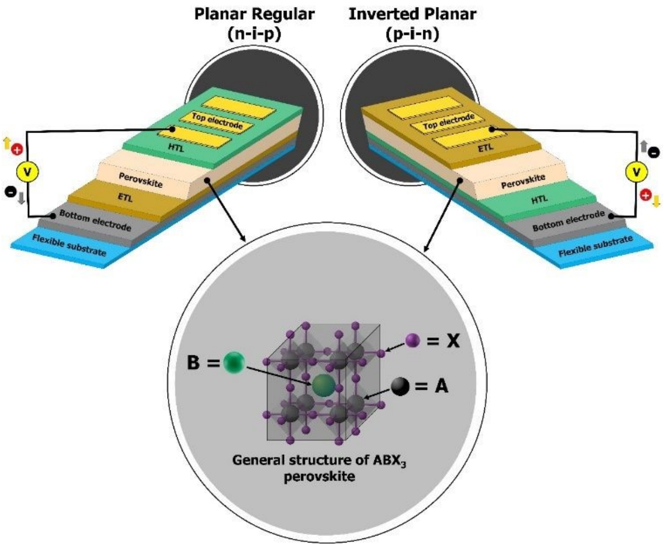

Figure 2. Schematic of Planar and Inverted Planar f-PeSCs for Indoor & Outdoor applications

3.1. History of perovskite solar cells

The evolution of solar cells, illustrated in **Figure 3**, reflects remarkable progress since 1839, as shown in **Figure 3a**, when Becquerel discovered the photovoltaic effect and the discovery of perovskite ($CaTiO_3$) in the same year, laying the foundations for the field [38,39]. In 1905, Einstein elucidated the photoelectric effect [40], and in 1954, Bell Labs created the first practical silicon solar cell [41]. In 1991, dye-sensitized cells (DSSC) emerged [42], and from 2009 onwards, with acceleration after 2018, f-PeSCs came to the fore. The PCE has evolved from less than 10% in 2012 to more than 40% under indoor conditions in 2024, combining high efficiency and flexibility. Between 2018 and 2024, f-PeSCs went through three phases: (1) 2018-2020, consolidation with PCEs of 15-18%, commercial testing and focus on encapsulation; (2) 2021-2023, optimization with PCEs above 20%, mechanical stability (>5000 cycles) and applications in BIPV and wearables; (3) 2024, advancements with indoor PCEs >40%, environmental stability (>90% after 1200h) and R2R processes reaching industrial maturity. In the future, integration with IoT, smart materials, storage, sustainability (lead-free perovskites, lower carbon footprint), transparent cells, and omnidirectional harvesting promises to expand the impact of f-PeSCs. **Figure 3b** presents one of the major challenges in the current scenario: balancing mechanical stability and environmental stability, highlighting how improvements over time contribute to both aspects [43]. Mechanical stability represents greater life cycle resistance and durability. Environmental stability indicates environmental resilience and long-term resistance to exposure to adverse conditions (such as humidity, temperature, and UV) [44]. Continued advancements in both areas are essential for optimized performance. Improvements in stability, with flex cycles increasing from hundreds to thousands and environmental resistance stretching from hours to thousands of hours, are being made through the use of self-healing materials and intelligent encapsulations.

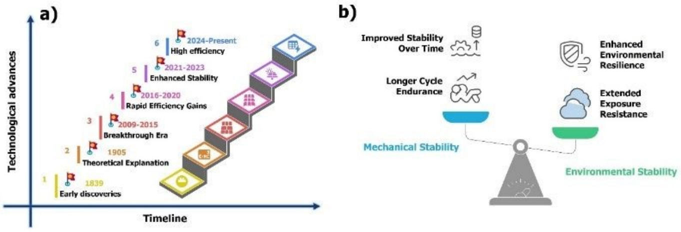

Figure 3. a) Advancing of the f-PeSCs technology; **b)** Balancing Stability in f-PeSCs

View Article Online
DOI: 10.1039/D5YA00363F

Figure 4a shows the historical trend of documents and citations from 1972 to 2024, which can be divided into three phases. In the gradual growth phase until 2010, the production of documents and citations remained low and grew slowly, increasing from 1 to 8 documents and from 0 to 43 citations, with sporadic activity until the 1990s and more noticeable growth from the 2000s onwards. From 2011 onwards, in the rapid progress phase from 2011 to 2017, there was a significant acceleration, with documents rising from 8 to 182 and citations growing from 43 to 5,981, highlighting an exponential growth that peaked in 2014, when documents increased by 150% (from 25 to 81) and citations increased by 152% (from 831 to 2,093). From 2018 onwards, in the tech advances phase, the trend evolved with sharp growth, documents rose from 253 to 563 (a growth of 122%) and citations from 9,380 to 27,463 (an increase of 193%), reflecting technological advances and massive impact, with documents growing 76% (from 320 in 2020 to 563 in 2024) and citations increasing 80% (from 15,271 to 27,463). **Figure 4b** shows the trend in documents from 2012 to 2024, along with a linear fit that predicts the future number of documents through 2030. The actual number of documents shows a steady increase, rising from 3 in 2012 to 563 in 2024. The linear fit, represented by the equation y = A + Bx and R^2 = 97.59%, closely follows the data, indicating a strong correlation. This suggests a consistent growth rate, with the model predicting ~605 documents by 2026 and ~800 by 2030, due to the emergence of these advances.

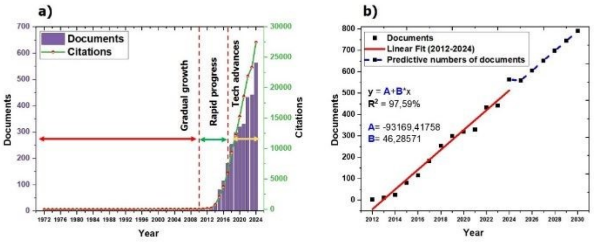

Figure 4. a) Historical Trend of Documents and Citations 1972-2024; and **b)** Linear Fit and Projections 2012-2030.

3.2. Technological Innovations of Energy Efficiency in f-PeSCs

Figure 5 presents the performance analysis and the most discussed topics in PeSCs between 2012 and 2024. **Figure 5a** shows the evolution of PCE efficiency (%) for f-PeSCs (black line) and r-PeSCs (red line). Based on data provided from for f-PeSCs (2012: 2.62% at Standard AM1.5G; 2013: 7% at Standard AM1.5G; 2015: 15.3% at Standard AM1.5G; 2016: 16.09% at Standard AM1.5G; 2017: 16.8% at Standard AM1.5G; 2018: 18.4% at Standard AM1.5G; 2019: 19.51% at Standard AM1.5G; 2020: 19.87% at Standard AM1.5G; 2021: 21.73% at Standard AM1.5G; 2022: 24.7% at Standard AM1.5G; 2023: 32.5% at 1000 lx; 2024: 41% at 1000 lx) [26,27,37,45–47,28–30,32–36]. And in the evolution of PCE for r-PeSCs with NREL efficiency data correspond to standard test conditions of (2012: 14.1%; 2013: 14.1%; 2014: 20.1%; 2016: 22.1%; 2017: 22.7%; 2018: 23.7%; 2019: 25.2%; 2020: 25.5%; 2022: 25.8%; 2023: 26.1%; 2024: 26.7%) [48]. It is observed that both cell types showed a gradual growth in PCE over the years. f-PeSCs show a more pronounced increase, reaching around 41% (to 1000 lx) in 2024, while r-PeSCs reach approximately 26.7% in the same period. This suggests significant advances in efficiency, especially for f-PeSCs. **Figure 5b** presents the seven most discussed topics in PeSCs, efficiency (31.35%), stability (26.65%), scalability (12.99%), cost (12.73%), flexible electrodes (10.84%), durability (3.91%) and sustainability (1.53%). It is worth noting that efficiency and stability are the most discussed topics, representing a significant proportion of the coverage, while durability and sustainability appear as the least discussed. This suggests that research and development in PeSCs has focused more on improving cell performance and reliability, with less emphasis on durability and sustainability, although these topics are emerging as promising areas in the field.

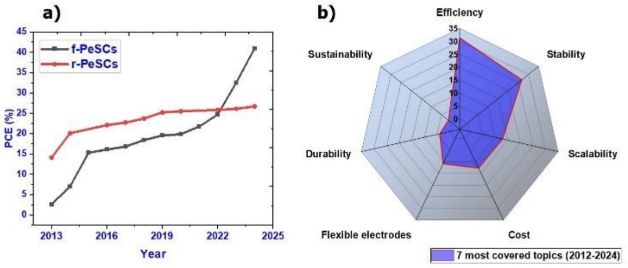

Figure 5. a) PCE in f-PeSCs and r-PeSCs from 2012-2024; and b) 7 Most Covered Topics in PeSCs

3.3. Technological scenario of the scientific field

Figure 6a shows the number of documents from various countries (A-J), with the highest contribution in 2019-2024. **Figure 6b** shows the percentage contribution by country (2012-2024): A: China (53.56%), B: United States (11.54%), C: South Korea (10.6%), D: India (5.14%), E: Hong Kong (4.2%), F: Australia (3.8%), G: Italy (3.14%), H: Japan (2.88%), I: Germany (2.88%), J (2.26%), led by China. **Figure 6c** displays the number of documents in research areas (A-J), with a significant increase in 2019-2024. **Figure 6d** shows the percentage

View Article Online
DOI: 10.1039/D5YA00363F

contribution by area (2012-2024): A: Materials Science (31.67%), B: Chemistry (17.3%), C: Engineering (14.45%), D: Physics & Astronomy (12.96%), E: Energy (10.04%), F: Chemical Engineering (7.15%), G: Biochemistry, Genetics & Molecular Biology (2.82%), H: Environmental Science (2.17%), I: Multidisciplinary (0.88%), J: Mathematics (0.56%), highlighting Materials Science and Chemistry. **Figure 6e** represents the number of documents in journals (A-J), with a notable increase in 2019-2024. **Figure 6f** presents percentage contribution by journals (2012-2024): A: ACS Applied Materials & Interfaces (20.99%), B: Advanced Functional Materials (13.7%), C: Advanced Materials (11.37%), D: Journal of Materials Chemistry A (10.69%), E: Nano Energy (9.62%), F: Chemistry of Materials (8.75%), G: Advanced Optical Materials (6.61%), H: Small (6.51%), I: Chemical Engineering Journal (5.93%), J: ACS Applied Energy Materials (5.83%), led by ACS Applied Materials & Interfaces and Advanced Functional Materials (Wiley).

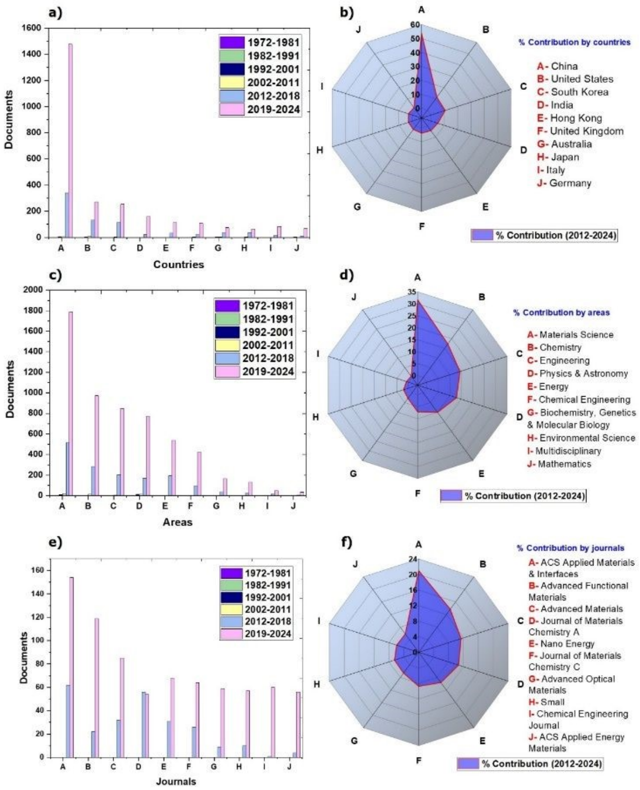

Figure 6. (**a**) Documents (1972-2024), and (**b**) % contribution by country (2012-2024); (**c**) Documents (1972-2024), and (**d**) % contribution by area (2012-2024); (**e**) Documents (1972-2024), and (**f**) % contribution by journal (2012-2024)

Figure 7 presents the number of documents published by keywords related to perovskites and associated technologies, divided into periods such as 1972-1981, 1982-1991, 1992-2001, 2002-2011, 2012-2018 and 2019-2024, including *Perovskite*, *Perovskite Solar Cells*, *Lead Compounds*, *Power Conversion*, *Solar Cells*, *Temperature*, *Efficiency*, *Halide Perovskites*, *Substrates* and *Photodetectors*. The sharp growth from 2012 onwards, especially between 2019 and 2024, with 2,772 publications for Perovskite (2,171 recent) and 1,341 for Perovskite Solar Cells (993 recent), reflects a significant advance in the technological landscape of the scientific field, highlighting the growing interest in perovskite materials and solar cells as innovative solutions for renewable energies. Before 2002, there were almost no records, with a modest increase until 2011 and a significant jump afterwards, suggesting that investments and innovations are shaping a new technological landscape, with a focus on efficiency and sustainability.

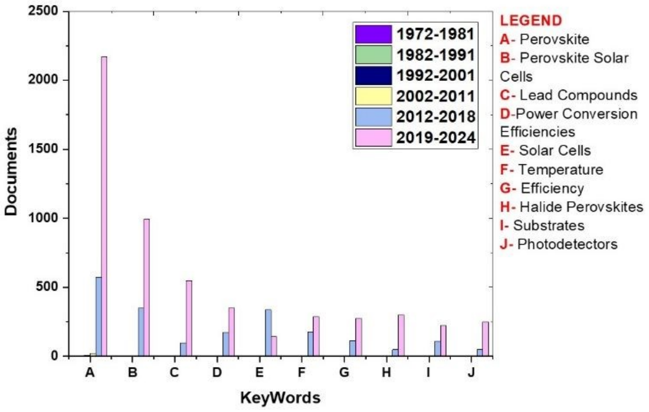

Figure 7. Documents published by keywords

Figure 8 shows a thermal map of keywords for 2012-2018 and 2019-2024, highlighting the frequency of terms about perovskites. In **Figure 8a**, *perovskite* and *perovskite solar cell* dominate, with *solar cells*, *flexible*, *low temperature*, and *stability* emerging, reflecting an initial focus on characterization and applications. In **Figure 8b**, *perovskite solar cell* persists, but *stability*, *flexible*, *efficiency*, *electron transport layer*, and *photovoltaics* gain prominence, indicating progress towards optimizing durability and efficiency, shaping a more sophisticated technological landscape in renewable energy. In **Figure 8c** (2012-2018), *Perovskite Solar Cells* (7.19%) and *Perovskite* (4.55%) lead, with *Flexible* (4.07%) and *Low Temperature* (1.68%) emerging, indicating an initial focus on solar cells and innovation. This distribution suggests that the initial focus was on exploring f-PeSCs and characterizing the materials, with emerging interest in flexibility and low-temperature processes, indicating the first steps towards practical and innovative applications. In **Figure 8d** (2019-

View Article Online
DOI: 10.1039/D5YA00363F

2024), *Perovskite Solar Cells* (18.93%) and *Perovskite* (17.17%) grow, *Stability* (10.94%) gains prominence, and *Flexible* (9.27%) advances, indicating a technological advance, with a focus on overcoming challenges such as stability and expanding flexible applications, shaping a more mature scenario focused on efficiency and commercial viability in renewable energy.

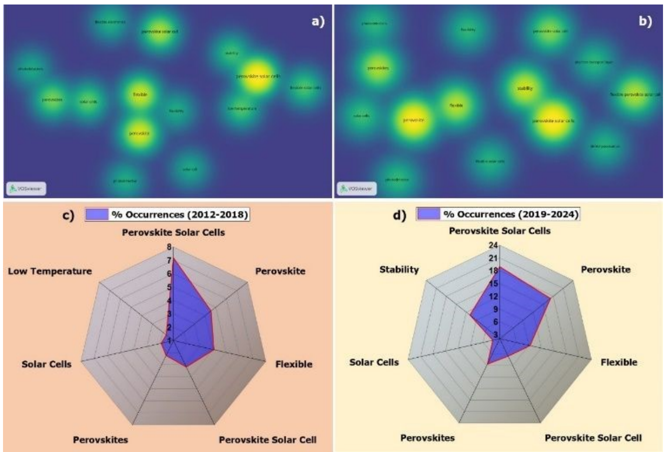

Figure 8. Thermal map of keyword frequency for f-PeSCs (**a**) in 2012-2018, and (**b**) in 2019-2024; % occurrences of terms (**c**) in 2012-2018, and (**d**) in 2019-2024.

3.4. Perovskite Solar Cell Market Segments

The projections in this section are based on international reports (Precedence Research, Cervicorn Consulting, IndustryARC, and Allied Market Research). They use compound annual growth rate (CAGR) models that consider government incentives, industrial expansion, and the demand for distributed energy harvesting. **Figure 9** shows the growth of the global solar cell and f-PeSC market in billions of US dollars (USD) from 2023 to 2034, reflecting the renewable energy technology landscape. In **Figure 9a**, the solar cell market grows from 149.45 billion in 2023 to 730.74 billion in 2034, with values such as 175.15 billion in 2025 and 531.99 billion in 2033, indicating a robust expansion due to investments and demand [49]. In **Figure 9b**, the f-PeSC market starts from 0.35 billion in 2023, reaching 8.81 billion in 2034, with 1.47 billion in 2028 and 7.15 billion in 2033, suggesting gradual but promising progress as f-PeSC technology gains relevance due to its efficiency and potentially low cost [50]. This highlights a scenario where traditional solar cells lead, but f-PeSCs emerge as a future innovation. A detailed overview of the global technology landscape in the field of solar energy, with a focus on f-PeSCs and PV capacity. **Figure 9c** presents a comparison of the market share of f-PeSCs and solar cells in four regions: North America, Europe, Asia Pacific, and LAMEA. Asia Pacific leads with 41% (f-PeSCs) and 48% (solar cells), indicating technological dominance [49,51]. North America follows with 28% (f-PeSCs) and 23% (solar cells), Europe with 22% and 21%, and LAMEA with 9% and 8%, suggesting less development. This highlights Asia Pacific as the epicenter of advancement in renewable energy. **Figure 9d** shows a projection of PV capacity in GW from 2023 to 2027: 1,552.3 GW (2023), 1,954.6 GW (2024), 2,776.3 GW (2025), 2,835.5 GW (2026), and 3,329.5 GW (2027) [52]. This growth reflects an accelerated expansion of solar infrastructure, driven by innovations such as f-PeSCs. The data indicate that Asia Pacific leads the development of solar technology, while global PV capacity is on track to triple, reinforcing the role of perovskites in advancing sustainability.

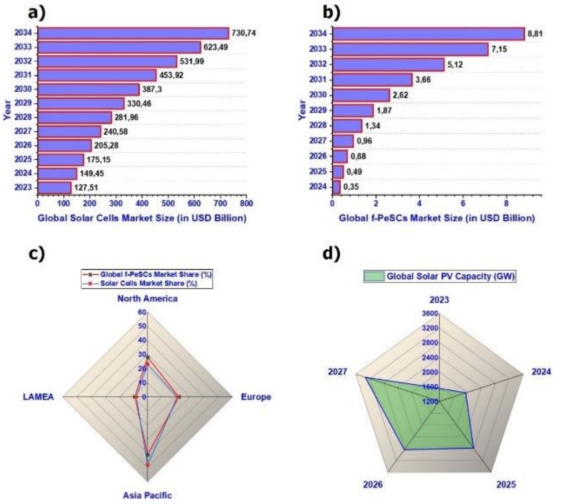

Figure 9. (**a**) Global solar cells, and (**b**) global f-PeSCs market size in USD billion; (**c**) Market share (%) of global f-PeSCs and solar cells; (**d**) Global solar PV capacity

4. Techniques, Flexible Substrates & Electrodes

f-PeSCs are emerging as a vital technology for the next generation of solar energy systems, especially those aimed at integration into portable, wearable, and curved-surface electronics. Their mechanical adaptability, lightweight structure, and potential for high efficiency under diverse lighting conditions make them attractive for both indoor and outdoor uses [53]. However, the design and performance of f-PeSCs heavily depend on three interconnected components: the fabrication techniques, the flexible substrate materials, and the choice of electrode configurations. To achieve stable and efficient energy conversion in flexible formats, it is crucial to tailor each layer

View Article Online
DOI: 10.1039/D5YA00363F

of the f-PeSCs to accommodate mechanical deformation while maintaining excellent optoelectronic performance. Compared to rigid solar cells, f-PeSCs must operate reliably under repeated bending, folding, or stretching [54]. This calls for careful selection of low-temperature, solution-processable methods and roll-compatible fabrication routes that preserve the intrinsic properties of perovskite materials.

In this section, we outline the major technological considerations for f-PeSCs development. First, we introduce key deposition and processing techniques compatible with flexible substrates. Then, we review the different classes of substrate materials that offer mechanical compliance and thermal stability. Finally, we discuss recent advancements in flexible electrode materials that are essential for efficient charge collection and device stability. These three components, techniques, substrates, and electrodes, serve as the structural and functional backbone of f-PeSCs. Their combined optimization is essential not only for improving device performance and longevity but also for enabling large-area, scalable production suitable for commercial deployment.

4.1. Techniques

The fabrication techniques used in f-PeSCs play a pivotal role in determining device performance, mechanical flexibility, and scalability. Since f-PeSCs must operate under physical deformation while retaining high photovoltaic efficiency, the methods employed for their deposition and assembly must be compatible with low thermal budgets, mechanically compliant materials, and R2R processing [55,56].

4.1.1. Solution-Based Processing

Solution-based methods, particularly spin-coating, are the most widely used techniques in laboratory-scale perovskite solar cell fabrication due to their simplicity, low cost, and precise control over film thickness and morphology. In f-PeSCs, spin-coating is primarily used for depositing the perovskite active layer and charge transport layers on flexible substrates such as polyethylene terephthalate (PET) or polyethylene naphthalate (PEN) [57]. However, spin-coating poses limitations for large-area production, prompting the adoption of alternative scalable methods.

4.1.2. Slot-Die Coating and Blade Coating

Slot-die and blade coating techniques are increasingly favored for producing uniform perovskite films over large areas. These methods are compatible with continuous R2R manufacturing and enable better control of film thickness and material utilization. Blade coating involves spreading a precursor solution across a heated substrate using a doctor blade, allowing for fine-tuning of crystallization kinetics by adjusting the temperature, blade speed, and solvent evaporation rate [58]. Similarly, slot-die coating (See **Fig. 10a**) uses a precision nozzle to deliver the solution onto a moving substrate, ideal for high-throughput production [59].

4.1.3. Inkjet and Spray Coating

Inkjet printing and spray coating (**Fig. 10b**, and **Fig. 10c**) are additive manufacturing techniques that offer material-efficient deposition and patterning capabilities. Inkjet printing is particularly advantageous for flexible and lightweight electronics because it enables precise, digital control of material placement, allowing for the fabrication of complex and customized device architectures [60]. Spray coating, on the other hand, allows uniform film formation on irregular or curved surfaces and is useful for applying transport layers and encapsulants [61].

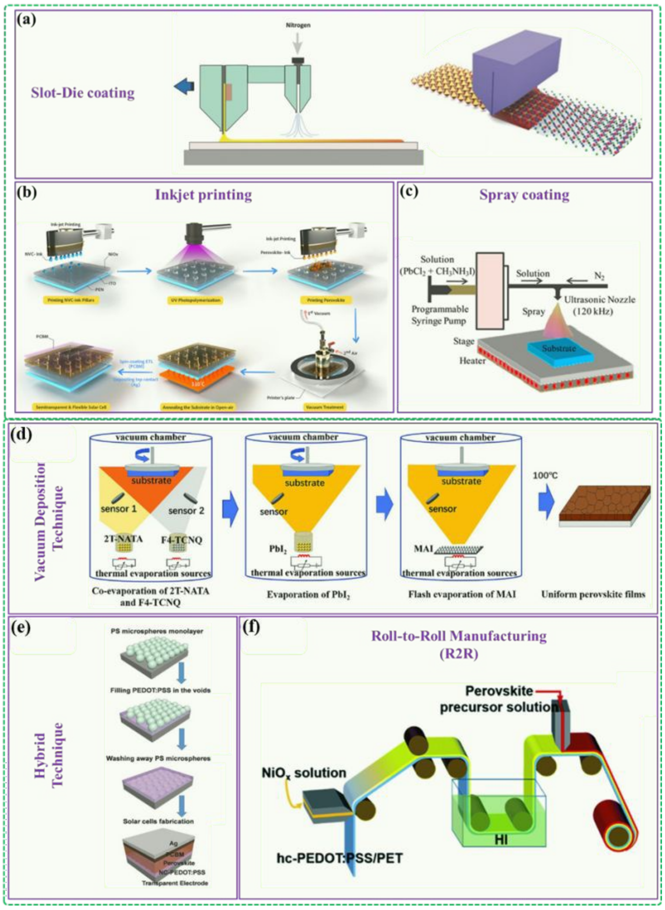

Figure 10. (**a**) Schematic depiction of slot-die coating incorporating a gas-quenching process. Reproduced with permission from Ref. [59], Copyright (2015), Wiley-VCH GmbH. (**b**) Schematic illustration of the key steps involved in the inkjet printing fabrication of a f-PeSCs.

View Article Online
DOI: 10.1039/D5YA00363F

Reproduced with permission from Ref. [60], Copyright (2023), Wiley-VCH GmbH. (**c**) Schematic illustration of the ultrasonic spray-coating process. Reproduced with permission from Ref. [61], Copyright (2015), American Chemical Society. (**d**) Co-evaporation under vacuum and formation of uniform perovskite films using a two-step evaporation–flash evaporation method. Reproduced with permission from Ref. [62], Copyright (2020), Wiley-VCH GmbH. (**e**) Schematic representation of the fabrication steps for nanocellular (NC) PEDOT:PSS scaffolds and their integration into perovskite solar cells. Reproduced with permission from Ref. [63], Copyright (2017), Wiley-VCH GmbH. (**f**) Schematic illustration of the fabrication process of perovskite solar cells using the R2R technique. Reproduced with permission from Ref. [64], Copyright (2021), The Royal Society of Chemistry.

4.1.4. Vacuum Deposition Techniques

While less common in f-PeSCs fabrication due to cost and equipment complexity, vacuum-based methods such as thermal evaporation (**Fig. 10d**) and sputtering are occasionally used to deposit electrodes (e.g., Au, Ag) and certain transport layers (e.g., MoO_3, ZnO). These techniques offer excellent control over film purity and thickness but are typically reserved for applications demanding higher device stability or integration with specific materials that are not solution-processable [62].

4.1.5. Hybrid and Tandem Fabrication Strategies

Emerging f-PeSCs architectures often incorporate hybrid fabrication methods that combine solution processing with vacuum deposition or use sequential deposition to construct multilayered or tandem devices. These approaches are particularly relevant for indoor energy harvesting and wearable electronics, where efficient operation under low-light conditions is crucial. Hybrid techniques also facilitate the integration of multiple absorber layers to extend spectral coverage and enhance power conversion efficiency (**Fig. 10e**) [63].

4.1.6. Roll-to-Roll Manufacturing

To transition from laboratory to industrial-scale production, R2R fabrication (**Fig. 10f**) stands as a promising strategy for f-PeSCs. R2R processes integrate coating, drying, annealing, and lamination steps in a continuous workflow, enabling high-throughput manufacturing of flexible photovoltaic modules. Compatibility with low-temperature and ambient atmosphere processing is key to implementing R2R methods for perovskite-based devices [64]. The choice of fabrication technique in f-PeSCs development is crucial for balancing efficiency, flexibility, and manufacturability. Scalable, low-cost, and low-temperature methods such as blade coating, slot-die coating, and inkjet printing are gaining prominence for commercial applications. As research advances, hybrid strategies and R2R approaches are expected to dominate the future landscape of f-PeSCs production. Among the manufacturing techniques discussed, blade coating, slot-die coating, and inkjet printing are considered the most promising for industrial-scale manufacturing. This is due to the compatibility of these techniques with roll-to-roll (R2R) processing and large-area deposition. In contrast, spin-coating remains limited to the laboratory environment, with low scalability. Although vacuum-based methods offer high-quality films, they significantly increase production costs. Therefore, the future industrial implementation of flexible perovskite solar cells should be based on hybrid approaches, combining large-area solution deposition with selective vacuum processing for critical layers.

4.2. Flexible Substrates

The substrate is a foundational component in f-PeSCs, influencing not only the mechanical properties and form factor of the device but also its processing conditions, environmental stability, and overall photovoltaic performance as shown in **Table 2**. Unlike conventional solar cells fabricated on rigid substrates such as glass, f-PeSCs require substrates that are thin, lightweight, and capable of withstanding repeated mechanical deformation without compromising electrical or structural integrity. An ideal flexible substrate for f-PeSCs must exhibit mechanical flexibility to withstand bending, folding, or stretching during operation and fabrication, while maintaining thermal stability to endure processing temperatures, typically below 150 °C, required for perovskite layer deposition and annealing. It should also possess chemical resistance to prevent interactions with solvents and precursor solutions during multilayer fabrication, ensure surface smoothness to support uniform coating of thin films and minimize interfacial defects, and provide optical transparency for semi-transparent or bifacial devices. Striking a balance between these properties is essential for achieving robust and efficient f-PeSCs, especially for integration into wearable electronics, portable power systems, and indoor applications.

Table 2. Comparison of flexible substrates used in f-PeSCs

Substrate	Thermal Stability	Optical Properties	Mechanical	Advantages	Limitations	Applications	Ref.

View Article Online
DOI: 10.1039/D5YA00363E

PET	70–80 °C	High transparency	Flexible	Low cost (~$2/kg), lightweight	Low thermal stability (60-70 µm/mK.)	Wearables, IoT PV	65
PEN	120 °C	High transparency	Stronger than PET	Better thermal stability (35-45 µm/mK)	Higher cost (~$8/kg)	Flexible PV modules, BIPV	65
PI	>300 °C	Moderate transparency	Excellent flexibility and mechanical robustness	Excellent thermal resistance (20-30 µm/mK)	Expensive (~$110 /kg),	Aerospace, high-temp electronics	65
Metal foil	>500 °C	Opaque	Very strong	Excellent barrier stability	Opaque surface	Outdoor PV, industrial devices	66–69

4.2.1. Polymeric Substrates

Polymeric films are the most common choice for flexible substrates due to their lightweight nature and excellent bendability. Among these, PET and PEN are widely employed. PET is one of the most extensively used flexible substrates in f-PeSCs due to its affordability, commercial availability, and compatibility with solution-based manufacturing techniques. It is optically transparent across the visible spectrum, which makes it well-suited for semitransparent devices and top-illumination configurations. PET films are lightweight and exhibit excellent dimensional uniformity, allowing for precise layer stacking and patterning. Despite these advantages, PET possesses a relatively low glass transition temperature (Tg) of approximately 70–80 °C. This thermal limitation restricts its application in processing conditions that require elevated temperatures, such as thermal annealing of the perovskite active layer or sintering of metal oxide electrodes (See **Fig. 11a**, and **Fig. 11b**) [70,71]. Exposure beyond this thermal threshold can lead to dimensional distortion, warping, or degradation of the polymer matrix, ultimately compromising device stability and performance. Furthermore, PET exhibits moderate barrier properties against moisture and oxygen, which are critical for the long-term operational stability of perovskite materials. To overcome this, PET is often coated with additional gas barrier layers such as atomic-layer-deposited (ALD) Al_2O_3 or sputtered SiO_2 to enhance its resistance against environmental degradation [72]. However, these added layers can increase complexity and cost, slightly reducing the appeal of PET for ultra-low-cost and disposable applications. Recent advances have focused on surface modification of PET films using plasma treatment or self-assembled monolayers (SAMs) to improve film wettability and adhesion with subsequent layers such as electron transport materials (ETMs) or hole transport materials (HTMs). This is crucial for uniform film formation and efficient charge extraction.

PEN is a polyester-based flexible substrate that shares many structural similarities with PET but offers improved thermal and mechanical properties. With a glass transition temperature in the range of 120–130 °C, PEN can withstand higher post-processing temperatures, enabling the fabrication of more thermally stable perovskite solar cells. This makes PEN a more attractive option for processes involving thermal annealing or the deposition of compact metal oxide layers that require temperatures above the tolerance limit of PET. PEN films exhibit high optical transparency in the visible spectrum and possess low water vapor transmission rates, offering better environmental barrier characteristics than PET. These properties make PEN suitable for applications requiring longer operational lifetimes or more demanding environmental exposure, such as outdoor integration (**Fig. 11c**, and **Fig. 11d**) [73,74]. However, PEN is relatively more expensive than PET and less widely available, which may limit its large-scale commercial application in cost-sensitive sectors. Additionally, like PET, PEN still requires surface treatments or barrier coatings to further improve moisture and oxygen resistance when used in ambient conditions. PEN has been used as a substrate for both planar and mesoporous perovskite solar cell architectures, showing reliable performance with R2R compatible processing techniques.

Polyimide (PI) stands out as one of the most promising polymeric substrates for f-PeSCs, particularly in applications requiring exceptional thermal and mechanical endurance. It exhibits a high glass transition temperature (typically >300 °C), excellent flexibility, and robust chemical resistance. These properties make PI highly compatible with various perovskite processing steps, including high-temperature annealing of both the perovskite absorber and interfacial layers, as well as the integration of durable electrode materials [75]. Unlike PET and PEN, PI can maintain structural integrity under significant thermal and mechanical stress, making it suitable for flexible electronics that undergo frequent bending or are exposed to fluctuating environmental conditions. PI substrates are also

View Article Online
DOI: 10.1039/D5YA00363F

dimensionally stable and exhibit minimal thermal expansion, which is essential for maintaining layer alignment and avoiding interfacial delamination during fabrication or operation. However, the primary limitations of PI are its relatively high cost and lower optical transmittance compared to PET and PEN. Most commercial PI films exhibit a characteristic yellow-brown tint, which reduces transparency and may limit their use in top-illuminated or semi-transparent PV applications [76]. This issue has been partly addressed through the development of optically clear PI films, although these remain less accessible due to cost and fabrication complexity.

Despite these constraints, PI's superior stability and mechanical robustness make it the substrate of choice for niche applications such as aerospace, wearable electronics, and advanced energy harvesting devices that demand long-term durability and high efficiency.

4.2.2. Metal Foils

Metal foils are widely explored as robust, flexible substrates for f-PeSCs, particularly in scenarios where mechanical strength, thermal stability, and environmental durability are essential. Commonly used metal foil materials include stainless steel, titanium, and aluminum, each offering distinct advantages based on application requirements. Stainless steel foils are the most frequently utilized due to their mechanical flexibility, excellent thermal tolerance (well above 500 °C), and low permeability to oxygen and moisture. These attributes allow stainless steel to serve as a reliable platform for processing high-performance perovskite layers and electrodes under ambient or elevated temperatures [77]. Moreover, their dimensional stability ensures minimal deformation during R2R processing or thermal cycling. A major benefit of metal foils lies in their inherent impermeability to environmental stressors such as water vapor and oxygen, which are known to degrade perovskite layers. This makes them especially attractive for outdoor applications where long-term operational stability is required. Additionally, their electrical conductivity allows the metal foil to double as a back electrode, potentially simplifying device architecture and reducing overall fabrication steps. Despite these advantages, metal foils are generally opaque, which limits their use to bottom-illumination or reflective-type device configurations. In most cases, a transparent conducting electrode must be deposited on the top side to enable photon absorption by the perovskite layer, as shown in **Fig. 11e**, and **Fig. 11f** [78]. Also, the rough surface morphology of untreated metal foils can hinder uniform layer deposition and introduce defects in the perovskite film. To overcome this, surface planarization techniques such as polishing, buffer layer deposition (e.g., TiO_2 or SnO_2), or polymer coatings are often employed to create a smooth and chemically compatible interface. Titanium foils, while less common, offer superior corrosion resistance and are lighter in weight compared to stainless steel. These are particularly suited for harsh environmental applications or niche areas like aerospace energy systems. Aluminum foils are lightweight and inexpensive, but they are more prone to corrosion and may require additional surface treatment or passivation to ensure chemical stability during device fabrication [79].

Metal foils provide a mechanically durable and thermally stable platform for f-PeSCs, with excellent resistance to environmental degradation. However, their opacity and surface roughness require careful consideration in device design and processing strategy.

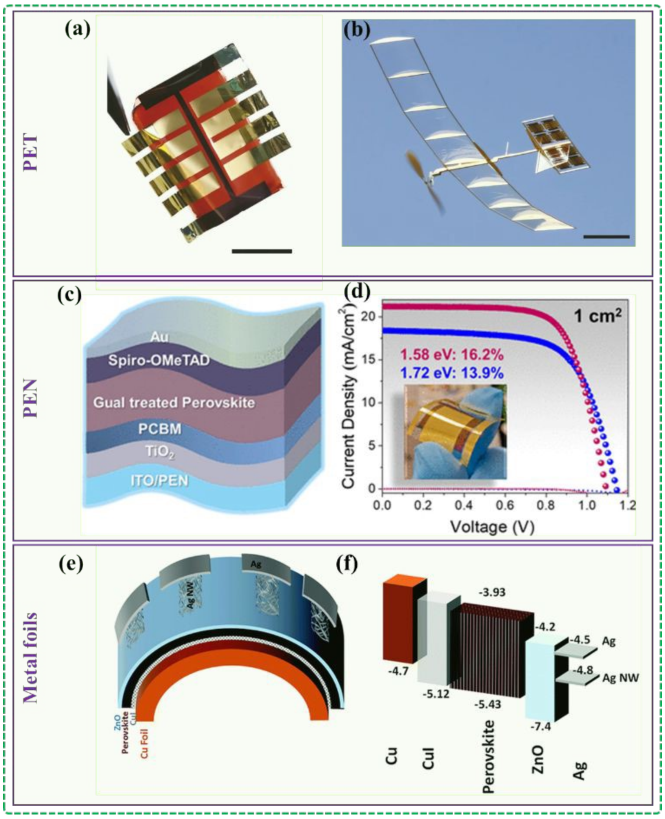

Figure 11. (**a**) Solar cell structure: 1.4 µm-thick PET foils act as the substrate, with PEDOT:PSS serving as the transparent hole-selective electrode. (**b**) Image capture of the model aircraft in flight during solar-powered outdoor operation. Reproduced with permission from Ref. [80], Copyright (2021), American Chemical Society. (**c, d**) Schematic representation and champion J–V characteristics of the flexible

View Article Online
DOI: 10.1039/D5YA00363F

perovskite solar cell. Reproduced with permission from Ref. [74], Copyright (2020), American Chemical Society. (**e**) Schematic diagram of the metal foil flexible perovskite solar cell and (**f**) Corresponding energy level alignment of the Cu/CuI/$CH_3NH_3PbI_3$/ZnO/Ag structure. Reproduced with permission from Ref. [78], Copyright (2017), The Royal Society of Chemistry.

4.2.3. Barrier-Coated Substrates

Barrier-coated substrates are an advanced class of flexible platforms that combine the mechanical flexibility of polymers with the environmental resistance of high-performance coatings. These substrates are especially critical for f-PeSCs, which are highly sensitive to moisture, oxygen, and UV light; factors that can rapidly degrade the perovskite layer and compromise device longevity. Barrier coatings are typically deposited on flexible base materials like PET, PEN, or PI to enhance their moisture and oxygen barrier properties, which are otherwise insufficient for long-term device stability. The most commonly used barrier layers include inorganic oxides such as aluminum oxide, silicon dioxide, and zinc oxide, as well as hybrid organic–inorganic multilayer coatings. These layers are deposited via ALD, plasma-enhanced chemical vapor deposition (PECVD), or sputtering, forming ultra-thin films that block gas permeation without significantly affecting flexibility or optical transmittance. One of the most promising developments in this area is the use of multilayer barrier architectures, in which alternating inorganic and organic layers are stacked to achieve ultra-low water vapor transmission rates (WVTR) in the range of 10^{-5} g/m^2/day: a level required for commercial-grade encapsulation of perovskite devices [81]. The organic interlayers (e.g., polymers like Parylene or epoxy-based resins) provide crack arresting properties and improve the flexibility of the entire structure, preventing brittle failure of the inorganic layers under bending or mechanical stress. These barrier-coated substrates provide extended device lifespan under ambient and accelerated aging conditions, compatibility with R2R processing essential for large-scale f-PeSCs production, high transparency ensuring efficient light absorption in front-illuminated configurations, and reduced encapsulation complexity, potentially lowering the need for external sealing layers. However, challenges remain. High-quality barrier deposition methods like ALD are often costly and time-consuming, which can limit scalability. Additionally, some barrier layers may not fully prevent ion migration from perovskite layers, a known issue affecting stability and performance over time. Research efforts are ongoing to develop low-cost, scalable alternatives such as solution-processed barrier coatings or laminated encapsulation films with comparable performance.

Barrier-coated substrates represent a strategic solution for extending the operational stability of f-PeSCs, particularly in humid or outdoor environments. Their integration into flexible solar modules is pivotal for bridging the gap between laboratory-scale efficiencies and real-world durability.

4.2.4. Emerging Substrate Materials

As the field of f-PeSCs evolves, new substrate materials are being developed to overcome the inherent limitations of conventional options like PET, PEN, or metal foils. These emerging substrates aim to combine flexibility, thermal stability, environmental resistance, optical transparency, and process compatibility: qualities that are critical for achieving long-term device performance across both indoor and outdoor applications. One promising direction is the use of biodegradable and eco-friendly substrates, such as cellulose nanofiber films, polylactic acid (PLA), and chitosan-based composites [82–84]. These materials are derived from renewable sources and are aligned with the growing demand for sustainable electronics. Though still in the early stages of development, they offer the potential for low environmental impact and disposability, particularly attractive for single-use or short-lifecycle electronic devices such as smart packaging, disposable sensors, or wearable healthcare patches. However, these substrates often require moisture-resistant coatings or encapsulation to protect the active layers from ambient degradation. Another exciting class of substrates includes ultrathin glass sheets, such as Willow Glass, which are manufactured to be both flexible and hermetically sealed [85]. These sheets can be bent to tight radii without cracking and offer exceptional barrier properties against moisture and oxygen, which is comparable to rigid glass, while retaining high optical transparency. Their thermal stability also allows high-temperature post-processing steps (>400 °C), which is crucial for some charge transport layers or crystallization steps in perovskite devices. However, the handling and processing of ultrathin glass require precision equipment due to their fragility at very thin dimensions (typically 50–100 µm).

Recent advances have also focused on composite substrates, where nanofillers such as graphene, boron nitride nanosheets, or ceramic particles are embedded within a polymer matrix to enhance thermal conductivity, gas barrier properties, or mechanical resilience [86,87]. These hybrid substrates are tailored to withstand harsh conditions while maintaining flexibility and

View Article Online
DOI: 10.1039/D5YA00363F

lightweight characteristics, making them ideal for specialized applications such as aerospace or high-temperature electronics.

Additionally, stretchable substrates like elastomers (e.g., PDMS, Ecoflex) are gaining attention for use in wearable photovoltaics. These materials can deform under mechanical stress and return to their original shape, enabling solar cells to conform to irregular or moving surfaces such as textiles, human skin, or robotic limbs. When combined with stretchable electrodes and encapsulants, they enable fully deformable solar modules, a key step toward next-generation soft electronics. However, achieving high efficiency on such platforms remains a significant challenge due to surface roughness and limitations in layer uniformity.

Emerging substrate materials offer novel pathways to enhance the sustainability, functionality, and application scope of f-PeSCs. While many are still under active research and optimization, their integration could lead to transformative advances in how and where solar energy can be harvested from skin-mounted devices to environmentally conscious disposable systems.

4.3. Flexible Electrodes

Flexible electrodes are essential components in f-PeSCs, enabling mechanical compliance without compromising electrical conductivity or interfacial stability as shown in **Table 3**. An ideal electrode must retain low sheet resistance, high optical transmittance (for transparent electrodes), chemical compatibility with adjacent layers, and mechanical robustness during bending, folding, or stretching. The choice of electrode materials directly affects device efficiency, long-term stability, and overall fabrication scalability.

Table 3. Comparison of flexible electrode materials

Electrode	Resistance (Ω/sq)	Optical Transmittance	Mechanical Flexibility	Key Limitation	Ref.
ITO	10-20	>90%	Low	Brittle behavior under bending	88,89
AZO	~10–38	80-85%	Moderate	Lower carrier mobility than ITO	90,91
Ag Nanowires	~10–15	>83–90%	High	Susceptible to oxidation and junction resistance	92,93
Graphene	~35–600	>90%	Very high	Higher sheet resistance compared with TCOs	94,95

4.3.1. Transparent Conductive Oxides (TCOs)

Transparent conductive oxides (TCOs) are among the most commonly employed materials for flexible electrode applications in f-PeSCs due to their unique combination of high optical transparency and electrical conductivity. These materials are typically deposited as thin films on flexible plastic substrates to serve as front electrodes, allowing light to reach the active layers while facilitating efficient charge extraction. The most prominent TCOs used in flexible devices include indium tin oxide (ITO), fluorine-doped tin oxide (FTO), aluminum-doped zinc oxide (AZO), and indium zinc oxide (IZO) [96].

4.3.1.1. Indium Tin Oxide (ITO)

ITO remains the benchmark TCO in photovoltaic research due to its excellent optoelectronic performance, offering transmittance above 85% in the visible range and sheet resistance as low as 10–20 Ω/□ when deposited under optimal conditions [97]. On flexible substrates such as PET or PEN, ITO can be deposited using techniques like radio-frequency (RF) sputtering or pulsed laser deposition (PLD). However, the use of ITO in f-PeSCs comes with several limitations. Most notably, its brittle nature causes the formation of microcracks under mechanical deformation, severely compromising conductivity and device performance under repeated bending or stress [98]. Studies have shown that the sheet resistance of ITO films can increase by over an order of magnitude when bent beyond small radii, rendering them unsuitable for highly flexible or stretchable applications.

Moreover, the high-temperature annealing (often above 200 °C) typically required to achieve low-resistance ITO layers is incompatible with most plastic substrates, which begin to soften or deform at relatively low glass transition temperatures (e.g., 70–120 °C for PET). While attempts have been made to deposit ITO at lower temperatures using modified sputtering conditions or post-treatment processes (such as UV annealing), these approaches often lead to films with inferior conductivity or poor adhesion to the substrate. In addition to mechanical fragility, resource scarcity and cost are concerns. Indium is a relatively rare and expensive element, leading to interest in replacing ITO with more sustainable alternatives that can offer comparable performance at lower cost and better mechanical compliance.

4.3.1.2. Fluorine-Doped Tin Oxide (FTO)

FTO is another widely used TCO, commonly utilized in rigid perovskite and dye-sensitized solar cells. While FTO exhibits superior

View Article Online
DOI: 10.1039/D5YA00363F

thermal and chemical stability compared to ITO, it is generally deposited on glass via spray pyrolysis or chemical vapor deposition at temperatures exceeding 400 °C, conditions unsuitable for plastic substrates. Moreover, FTO films tend to be thicker and rougher, limiting their applicability in thin, flexible architectures where smooth interfaces are necessary for optimal layer stacking [99]. Attempts to deposit FTO at lower temperatures using sol-gel or other solution-based methods have been explored, but such films often display lower electrical conductivity and poorer uniformity over large areas, making them less favorable for f-PeSCs.

4.3.1.3. *Aluminum-Doped Zinc Oxide (AZO) and Indium Zinc Oxide (IZO)*

As alternatives to ITO and FTO, AZO and IZO have gained attention for their abundance, tunable electrical properties, and better adaptability to low-temperature deposition processes. AZO, in particular, can be deposited by sputtering, spray pyrolysis, or sol-gel methods at temperatures as low as 150–200 °C, making it more compatible with flexible substrates. Additionally, zinc and aluminum are both earth-abundant and low-cost materials, offering a more sustainable pathway for TCO development. IZO, being a mixed metal oxide, combines the high conductivity of indium-based materials with enhanced flexibility due to its amorphous nature [100]. This allows IZO to maintain performance under mechanical deformation better than ITO, though its dependence on indium still raises concerns regarding long-term availability and cost.

Despite these promising characteristics, AZO and IZO films typically show higher resistivity and lower carrier mobility than ITO, particularly when processed at low temperatures. Surface roughness and film uniformity are also critical issues to address when integrating these TCOs into multilayer f-PeSCs.

4.3.1.4. *Processing and Integration Challenges*

For TCOs to be viable in f-PeSCs fabrication, they must be compatible with solution-processed layers, provide good adhesion, and exhibit chemical stability under ambient and encapsulated conditions. Additionally, TCOs should not chemically react with or diffuse into adjacent functional layers during fabrication or operation, which could deteriorate device performance or induce hysteresis in the current-voltage characteristics. Flexible substrates impose further constraints due to their thermal and mechanical limitations. Thus, low-temperature TCO deposition methods are essential, including room-temperature sputtering, solution processing, and ALD using low-temperature precursors. However, each of these techniques involves trade-offs between film quality, processing speed, equipment cost, and environmental impact.

4.3.1.5. *Strategies for Enhancing TCO Performance*

To address the mechanical fragility of TCOs, especially ITO, researchers have developed strategies including laminating TCOs onto elastomeric substrates to absorb mechanical stress, embedding TCOs in polymer matrices to enhance crack resistance, and coating TCOs with flexible buffer layers such as conductive polymers or graphene to reduce strain during bending. Additionally, composite or hybrid TCO layers are being developed by incorporating nanostructured materials (e.g., silver nanowires, CNTs, or graphene flakes) to create flexible, conductive, and transparent electrodes that outperform traditional TCOs under mechanical deformation [76].

While TCOs such as ITO, FTO, AZO, and IZO remain vital to f-PeSCs development, their integration into mechanically flexible platforms is limited by processing conditions, mechanical brittleness, and resource availability. Continued research into low-temperature deposition, hybrid structures, and alternative materials is critical for the next generation of durable, scalable, and cost-effective transparent electrodes in flexible solar technologies.

4.3.2. Metallic Nanostructures

Metallic nanostructures have emerged as highly promising alternatives or complements to traditional TCO electrodes in f-PeSCs due to their excellent electrical conductivity, optical transparency, and superior mechanical flexibility. These nanostructured electrodes typically consist of networks or meshes made from nanoscale metal wires, grids, or nanoparticles, which provide continuous conductive pathways while allowing light to pass through the spaces between the metallic elements.

4.3.2.1. *Types of Metallic Nanostructures*

Silver Nanowires (AgNWs), among metallic nanostructures, are the most extensively studied for flexible electronics and photovoltaics. They offer a unique combination of low sheet resistance (down to 10 Ω/□) and high optical transmittance (>85%) in the visible spectrum. AgNWs can be deposited via solution processing methods such as spin coating, spray coating, or R2R printing, making them highly compatible with scalable, low-cost fabrication [101]. Their intrinsic flexibility allows them to withstand bending, stretching, and folding better than brittle TCOs like ITO. Copper Nanowires (CuNWs) are gaining traction as a low-cost alternative to AgNWs due to the abundance and lower price of copper. However, CuNWs are more prone to oxidation, which degrades their conductivity over time.

View Article Online
DOI: 10.1039/D5YA00363F

Recent advancements in surface passivation and encapsulation techniques have improved their environmental stability, making them more viable for f-PeSCs applications [102]. Metallic meshes and grids, formed by the patterned deposition of metals such as silver, gold, or copper, provide highly conductive and transparent electrodes. These can be fabricated via photolithography, nanoimprint lithography, or self-assembly methods. The mesh structures are particularly attractive for flexible devices, as their open geometry reduces mechanical strain during bending, thereby maintaining conductivity even after repeated deformation cycles [103]. Metallic Nanoparticle Networks, constructed from metal nanoparticles linked together, can also serve as flexible electrodes. However, these typically require post-deposition sintering or annealing to achieve sufficient conductivity, which poses challenges for temperature-sensitive flexible substrates [104].

4.3.2.2. Advantages of Metallic Nanostructures

Metallic nanostructures in f-PeSCs offer several advantages. Unlike brittle TCO films, metallic nanowire networks provide mechanical flexibility, enduring large bending radii and repeated flexing without significant resistance increases due to their percolative network, which allows nanowires to reorient or slide under strain. They also enable scalability and low-cost fabrication through solution-based deposition techniques, facilitating large-area coating of flexible substrates compatible with R2R manufacturing processes essential for commercial viability. Additionally, optimized metallic nanowire films achieve high conductivity with sheet resistances comparable to or better than ITO while maintaining high optical transparency, crucial for efficient light harvesting in f-PeSCs.

4.3.2.3. Challenges and Solutions

Metallic nanostructures, despite their advantages, face several challenges. Surface roughness in nanowire networks, often caused by protruding junctions, can lead to shunting or damage to active layers deposited above. This issue can be mitigated by embedding nanowires in a planarizing polymer layer or applying conductive overcoats, such as PEDOT:PSS or graphene, to smooth the electrode surface. Chemical stability is another issue, as metals like silver are prone to oxidation and sulfurization, which reduces conductivity over time. Protective encapsulation layers or chemical treatments, such as thiol ligands or graphene coatings, have been developed to enhance long-term stability under ambient conditions. Additionally, contact resistance at junctions between overlapping nanowires can limit overall conductivity. However, techniques such as thermal annealing, mechanical pressing, or chemical welding can reduce these resistive junctions to improve electrode performance. Finally, while silver offers excellent properties, its high cost drives the exploration of alternatives, such as copper or nickel nanowires; however, ensuring their long-term stability and oxidation resistance remains an active research area. Metallic nanostructures represent a versatile and effective class of flexible electrodes for f-PeSCs. Their combination of mechanical robustness, excellent conductivity, and optical transparency offers a compelling alternative to brittle TCO films. Addressing the challenges of surface roughness, stability, and scalability through innovative material design and processing techniques will be key to their widespread adoption in next-generation flexible solar technologies.

4.3.3. Carbon-Based Electrodes

Carbon-based electrodes have garnered significant interest as promising alternatives to traditional transparent conductive materials in f-PeSCs. Their inherent advantages such as low cost, chemical stability, mechanical robustness, and compatibility with low-temperature processing, make them well-suited for flexible and wearable photovoltaics. These electrodes can be integrated in various forms, including carbon nanotubes (CNTs), graphene, carbon black, and even printable carbon pastes.

4.3.3.1. Carbon Nanotubes (CNTs)

CNTs, especially single-walled (SWCNTs) and multi-walled (MWCNTs), offer high electrical conductivity and excellent mechanical flexibility. Their 1D nanostructure enables the formation of conductive networks that can maintain their performance under mechanical strain, such as bending or twisting (**Fig. 12a**). CNT-based electrodes can be deposited through solution-based methods (e.g., spray coating, drop-casting, or vacuum filtration), allowing integration with large-area flexible substrates. Studies have demonstrated that CNTs not only serve as top electrodes but also aid in efficient hole extraction in perovskite layers [105,106]. Moreover, they can replace expensive and brittle materials like ITO or metal back contacts, reducing both cost and complexity. Challenges include the need for uniform dispersion in solvents, high sheet resistance at low densities, and potential interfacial mismatches with the perovskite layer. Functionalization and doping strategies are being explored to overcome these limitations.

4.3.3.2. Graphene and Derivatives

Graphene, an atomically thin, two-dimensional form of carbon, possesses remarkable electrical and mechanical properties. It is

View Article Online
DOI: 10.1039/D5YA00363F

highly transparent and flexible, making it an excellent candidate for transparent electrodes in f-PeSCs (**Fig. 12b**). Graphene can be prepared using CVD or solution processing. In f-PeSCs, monolayer or few-layer graphene sheets can act as both the conductive top layer and a protective barrier against moisture and oxygen [107]. However, pristine graphene has relatively high sheet resistance compared to conventional TCOs. Efforts to reduce resistance include chemical doping, hybridization with other conductive materials (e.g., AgNWs or CNTs), and developing multilayer configurations. Additionally, reduced graphene oxide (rGO), derived from the reduction of graphene oxide, offers an economical and scalable route for producing carbon-based electrodes, albeit with lower conductivity than pristine graphene [108].

4.3.3.3. Carbon Black and Printable Carbon Pastes

Carbon black and graphite-based pastes are often used as printable back electrodes in f-PeSCs. These carbon electrodes are particularly advantageous in simplifying device architecture since they can be printed directly onto perovskite layers without requiring vacuum deposition or metallic contacts (**Fig. 12c**). Moreover, these electrodes exhibit high stability under humidity and thermal stress, making them attractive for outdoor flexible devices. Printable carbon electrodes have been successfully used in hole-conductor-free perovskite devices, significantly lowering manufacturing costs [109]. However, their application in front electrodes remains limited due to their low transparency. Nevertheless, they are being increasingly integrated into semi-flexible modules for niche applications like packaging-integrated PV or wearable patches.

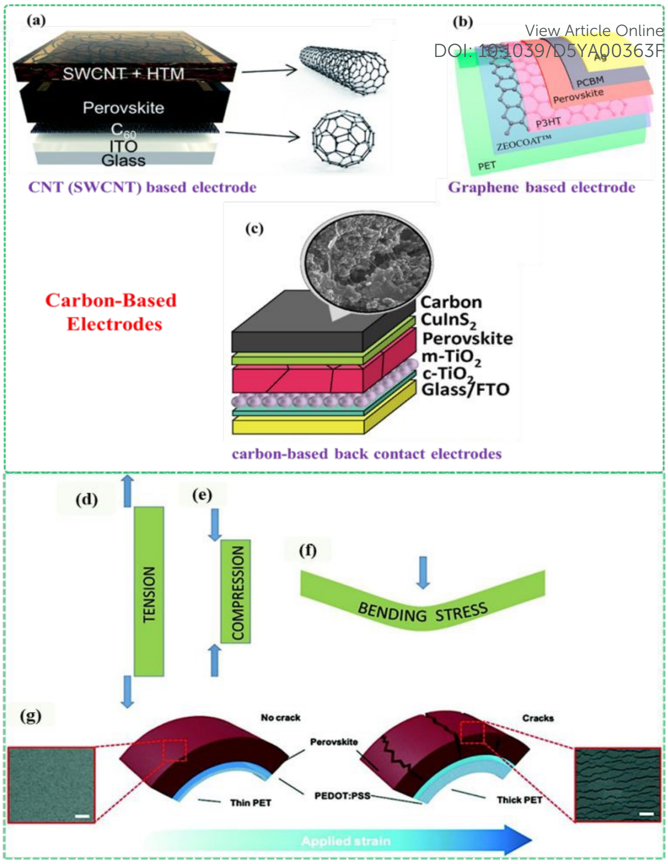

Figure 12. (**a**) Graphical illustration of flexible perovskite solar cells with a sandwich structure incorporating SWCNTs and C_{60} layers. Reproduced with permission from Ref. [106], Copyright (2018), The Royal Society of Chemistry. (**b**) Schematic illustration of a flexible perovskite solar cell featuring the layered structure: PET/graphene/P3HT/perovskite/$PC_{71}BM$/Ag. Reproduced with permission from Ref. [107], Copyright (2016), Elsevier. (**c**) Layered structure schematic of the device: FTO/TiO_2-compact/mesoporous TiO_2/perovskite/$CuInS_2$/carbon. Reproduced with permission from Ref. [109], Copyright (2024), Elsevier. Schematic representation of common mechanical stress types affecting perovskite layers: (**d**) tensile stress, (**e**) compressive stress, and (**f**) bending stress. (**g**) Illustrates potential failure modes such as interfacial delamination and microcrack formation under mechanical loading. Reproduced with permission from Ref. [110], Copyright (2025), Elsevier.

4.3.3.4. Advantages and Challenges of Carbon-Based Electrodes

Carbon materials offer mechanical resilience, making them ideal for flexible devices that undergo frequent deformation. They are low-cost and abundant on Earth compared to rare elements like indium

View Article Online
DOI: 10.1039/D5YA00363F

used in ITO. Most carbon-based electrodes exhibit excellent chemical stability, resisting degradation in humid, thermal, and UV environments, which enhances device longevity. Additionally, carbon materials can often be processed under ambient conditions using R2R compatible techniques, unlike metal-based electrodes that require high vacuum or high-temperature conditions. However, carbon-based electrodes face challenges that must be addressed for widespread application. Both CNT and graphene-based electrodes can have higher sheet resistance than TCOs, negatively impacting device performance, which necessitates optimization through doping and hybrid structures. Achieving optimal charge transfer at the carbon–perovskite interface requires careful engineering of interlayers or surface functionalization. While lab-scale demonstrations are promising, translating these technologies to large-area modules demands reproducible and uniform coating methods. Emerging research is exploring carbon–metal hybrid electrodes, combining the conductivity of metals with the flexibility and chemical robustness of carbon materials. Such combinations aim to achieve the best of both worlds in future f-PeSCs applications. Carbon-based electrodes present a compelling route toward cost-effective, stable, and flexible perovskite solar cells. Their tunable properties, compatibility with solution processing, and mechanical robustness make them key contenders for next-generation energy harvesting technologies, especially in indoor, wearable, and portable device markets.

5. Key Challenges & Solutions in applications

Flexible perovskite solar cells have emerged as a promising alternative to conventional rigid solar technologies. For both indoor and outdoor applications, f-PeSCs possess several advantageous performance properties that make them suitable for various applications. In contrast to silicon-based photovoltaics, which are rigid, heavy, and expensive to manufacture, f-PeSCs are perovskite materials that possess excellent optoelectronic properties while remaining flexible and lightweight [111]. These advantages can be applied to curved surfaces, allowing f-PeSCs to be building-integrated photovoltaics (BIPV), vehicle-integrated photovoltaics (VIPV), wearable electronics, and IoT devices [80,112]. Perovskite is compatible with low-temperature processing for f-PeSCs, enabling them to be deposited on PET or PEN, further enhancing their adaptability in diverse environments [113]. However, although many advantages can be realized, f-PeSCs have environmental, mechanical, and scalability limitations and face performance optimization problems under different lighting conditions [114]. It is therefore essential to scale up the f-PeSC technology toward commercial viability and widespread adoption across various industries.

5.1. Stability Issues of f-PeSCs in Outdoor Environments

A significant challenge that impedes the long-term viability of f-PeSCs in an outdoor environment is the device's deterioration, caused by factors associated with degradation, such as humidity, heat, ultraviolet radiation, and cycling between cold and hot temperatures. Among these factors, humidity is one of the most detrimental, defined as a critical degradation factor, as it precipitates chemical reactions in the perovskite layer, forming hydrated phases such as $MAPbI_3 \cdot H_2O$, which significantly reduce the performance of the photovoltaic device [115]. Studies have shown that increasing humidity levels can reduce the power conversion efficiency of PCE by 20–30% after only 1000 hours of operation under standard light conditions AM 1.5G, 100 mW/cm^2 [14]. Furthermore, high temperatures intensify instability, especially in methylammonium lead iodide ($MAPbI_3$)-based perovskites, where phase transitions and thermal decomposition occur above 60 °C, resulting in irreversible efficiency losses [116,117]. UV radiation accelerates the degradation rate through photoinduced oxidation, reacting with the perovskite layer and hole-transport materials, and reducing PCE by 65% in the first weeks when combined with exposure to humidity [118,119]. Thermal cycling, resulting from diurnal temperature fluctuations to which f-PeSCs will be subjected in the external environment, adds mechanical stress to material interfaces, generating delamination and microcracks that compromise the device's integrity [120]. Collectively, these factors significantly restrict the operational lifetime of f-PeSCs, underscoring the need for the effective development of advanced encapsulation techniques, stable perovskite formulations, and sustained protective coatings to enable sustainable operation in outdoor environments.

5.2. Mechanical Durability of f-PeSCs Under Bending Stress

The mechanical durability of f-PeSCs is a critical factor determining their suitability for dynamic outdoor applications such as foldable chargers, VIPV, and portable solar panels. Repeated bending and flexing induce mechanical stress that can lead to microcracks in the perovskite layer, charge transport layers, and electrodes, ultimately causing efficiency losses ranging from 15% to 25% after approximately 2000 bending cycles with a curvature radius of 3.5 mm

View Article Online
DOI: 10.1039/D5YA00363F

[99,121,122]. This degradation primarily arises from strain accumulation at grain boundaries within the perovskite film, increasing defect density and facilitating moisture ingress, which further accelerates material breakdown [123]. Additionally, large-scale f-PeSCs installations in BIPV may experience wind-induced flexing, exacerbating mechanical fatigue over time [124,125]. With the growing interest in f-PeSCs, the focus on their mechanical durability has intensified. This durability pertains to the material's capacity to resist cracking and structural deformation due to external mechanical forces, such as bending or twisting, as well as residual stresses from thermal annealing processes. High processing temperatures can impose strain on flexible plastic substrates, potentially resulting in defects within the perovskite layer. Elastomeric materials are particularly beneficial in these applications because they can revert to their original shape once the mechanical stress is alleviated. The primary mechanical stresses encountered include tensile stress (**Figure 12d**), compressive stress (**Figure 12e**), and bending stress (**Figure 12f**). Under sustained mechanical strain, stress accumulates within the device layers, often leading to crack formation, which is a key degradation mechanism. Stress concentrations are typically found at grain boundaries, material defects, and interfacial regions, where microcracks initiate and propagate over time. As these cracks expand with repeated loading, they disrupt electrical continuity, impede charge transport, increase non-radiative recombination, and ultimately lead to a marked decrease in PCE. In addition to crack formation, interfacial delamination, as seen in **Figure 12g**, represents another critical mechanical failure mechanism in perovskite solar cells. This occurs when adjacent layers, such as the perovskite absorber and the charge transport or electrode layers, separate at their interfaces. The fundamental factors include weak interfacial bonding, incompatible mechanical properties between different layers, or pre-existing defects at the interface. Once debonding is triggered, it can spread rapidly under repeated mechanical stress, resulting in widespread cracking, layer peeling, and the formation of voids. This structural failure compromises both electrical connectivity and the device's waterproofing against environmental exposure. Because of this, cracking and debonding of solder cells often work together to accelerate overall degradation. Researchers have suggested several ways to mitigate these effects, including the addition of polymeric additives that increase crystallinity and crack resistance. f-PeSCs can maintain 75–90% of their PCE after 3000–10000 bends with a bend radius of 3–5 mm [126,127]. Self-healing polymers, such as hyperbranched polymers with hydrogen bonding networks that self-heal microcracks during repeated bending, maintaining 95% PCE after 5000 bending cycles [128]. In addition, transparent conductive electrodes containing silver nanowires and graphene exhibit much greater mechanical resilience than brittle indium tin oxide (ITO), preserving conductivity and minimizing efficiency loss under continuous flexing [129,130]. To enhance the mechanical durability of f-PeSCs under high-humidity conditions, a bioinspired hyperbranched polymer dopamine adhesive (HPDA) was developed. Drawing inspiration from marine mussels, which adhere strongly to surfaces underwater through adhesive proteins containing dopamine (DOPA), HPDA incorporates dopamine end groups that facilitate robust adhesion even in humid environments. Unlike conventional linear polymers, hyperbranched polymers (HBPs) offer a three-dimensional architecture with numerous functional end groups, thereby enhancing both flexibility and mechanical strength. As illustrated in **Figure 13a**, HPDA effectively binds to perovskite grains and interfaces, reinforcing grain boundaries and forming a vertical scaffold throughout the film. The oxygen-containing groups in HPDA coordinate with Pb^{2+} ions, suppressing crack initiation and propagation. Additionally, HPDA strengthens the interfaces between the perovskite layer and both the electron transport layer (SnO_2) and hole transport layer (spiro-OMeTAD), significantly improving interfacial toughness. **Figure 13b** and **Figure 13c** demonstrate HPDA’s strong and stable adhesion to ITO sustrates, even after water exposure, while FTIR and XPS analyses (**Figure 13d** and **Figure 13e**) confirm the chemical interactions between HPDA and the perovskite layer. This multifunctional adhesive system effectively mitigates humidity-accelerated mechanical degradation, paving the way for highly efficient and durable f-PeSCs. Advanced structural designs, such as kirigami-inspired architectures and adhesive polymer interlayers, further enhance mechanical robustness by distributing stress more evenly across the device, reducing delamination risks and extending operational longevity [131]. These advancements collectively contribute to improving the mechanical durability of f-PeSCs, ensuring reliable performance in demanding outdoor environments.

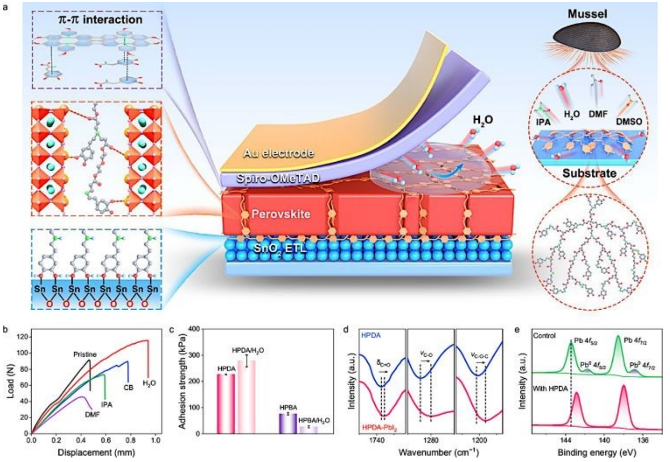

Figure 13. (**a**)Schematic showing the underwater adhesion mechanism of natural mussel-inspired HPDA in perovskite films (**b**) Lap shear strength of HPDA on ITO under various solvent conditions. (**c**) Adhesion strength comparison of HPDA and HPBA on ITO after water washing (n = 3, error bars: SD). (**d**) FTIR spectra of HPDA and HPDA–PbI_2 films. (**e**) XPS Pb 4f spectra of pristine and HPDA-treated perovskite layers. Reproduced with permission (CC BY license) from Ref. [132], Copyright (2025), Nature.

5.3. Scalability Challenges and Manufacturing Techniques for f-PeSCs

Although the performance shown by f-PeSCs in laboratory-scale demonstrations has been remarkable, manufacturing efforts for industrial production remain challenging. Conventional methods such as spin-coating, although successful in research settings, are ineffective for deposition over large areas, as valuable material is wasted and film districts are unevenly covered, resulting in efficiency losses of up to 10–20% for larger devices [131,133]. Furthermore, achieving high-quality perovskite film over large areas remains a critical issue, since defects such as pinholes and uneven thickness reduce device performance and reliability [134]. As a solution to these limitations, several large-scale fabrication techniques, such as R2R printing, slot-die coating, inkjet printing, and vapor-assisted deposition, have been investigated to enable the fabrication of more efficient and cost-effective f-PeSCs suitable for commercialization [135]. R2R printing has emerged as a promising solution for the mass fabrication of f-PeSCs, as it provides the ability to rapidly deposition them over large areas on flexible substrates while maintaining uniformity and reproducibility [136]. A snapshot of the R2R process is given in **Figure 14**. Previous studies have shown that R2R-compatible perovskite formulations enable f-PeSCs with PCE ranging from 12% to 14% over active areas of more than 10 cm^2 [137]. Slot-die coating, on the other hand, is another scalable fabrication technique that enables recent control over the deposition of the perovskite precursor, forming a high-quality film with minimal defects [138]. For example, work conducted at King Abdullah University of Science and Technology (KAUST) demonstrated slot-die coated f-PeSCs tandem modules with a PCE of 13.8% over an area of 50 cm^2, showing the viability of the technique for large-scale deployment [139]. Inkjet printing, moreover, offers additional benefits in deposition patterning and material consumption reduction, which makes it attractive for customized applications such as full-surface BIPV and wearable electronics [140,141]. Recent advancements have shown that inkjet-printed perovskite films can maintain high PCEs while reducing material usage by up to 30%, demonstrating its potential for large-scale implementation [142]. In addition to solution-based techniques, vacuum-assisted deposition methods have been investigated to achieve high-quality perovskite films with improved crystallinity and fewer defects [143]. Vapor-assisted approaches, such as dual-source evaporation and flash evaporation, have enabled the fabrication of f-PeSCs with PCEs exceeding 10-23% over 16-100 cm^2 devices, showcasing their compatibility with industrial-scale manufacturing [144]. Combining solution and vapor-phase techniques has further enhanced film morphology, resulting in f-PeSCs with PCEs of 22.8-24.1% over 0.1 cm^2 while retaining 95% of their initial efficiency after 20000 hours of ambient exposure [144,145]. The use of green solvents, such as 2-methoxyethanol, has also contributed to reducing defects in large-area films, improving processability and environmental sustainability [146,147]. As these scalable manufacturing strategies continue to evolve, they hold the potential to drive f-PeSCs toward commercialization, enabling cost-effective solar solutions for both indoor and outdoor applications [148].

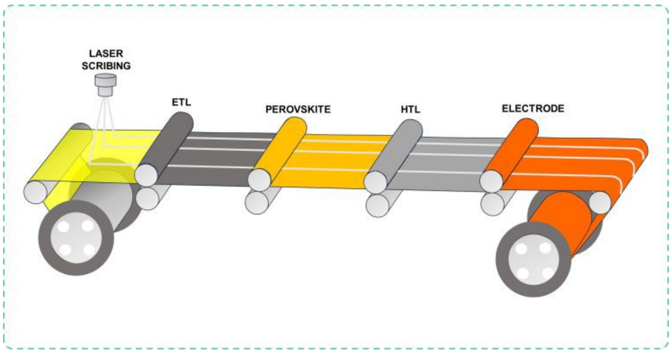

View Article Online
DOI: 10.1039/D5YA00363F

Figure 14. In-line R2R processing of all layers of f-PeSCs for fabrication of Flexible Devices.

5.4. Performance of f-PeSCs in Indoor Lighting Conditions

The f-PeSCs have demonstrated remarkable efficiency in indoor lighting environments, making them ideal for powering low-power electronic devices such as sensors, wearables, and IoT applications. Unlike silicon-based solar cells, which suffer from impaired performance at low light levels, f-PeSCs benefit from their tunable bandgap structure, which enables them to efficiently absorb photons in the visible spectrum range of 400–700 nm, typically emitted by artificial light sources such as LED and fluorescent lamps [15]. Recent studies have shown that f-PeSCs can achieve PCEs of over 30% under indoor lighting levels ranging from 100 to 1000 lux, significantly outperforming the efficiency of existing photovoltaic technologies under these conditions [18]. This feature is especially desirable for indoor applications where direct solar energy is not accessible, and the only available energy source is indoor ambient light. Several reasons underlie the improved performance of f-PeSCs in indoor environments, including their effectiveness when operating at low irradiance levels, their compatibility with flexible substrates, which makes them ideal for integrating compact electronic systems, and the ability to be designed to match specific light spectra [149]. Mixed halide perovskites are designed with compositions tuned to optimize light absorption at wavelengths corresponding to warm-white LED light, which improves the efficiency of f-PeSCs in real indoor environments [150]. Furthermore, recent innovations in electron-transporting material and hole-transporting materials have improved charge extraction and reduced recombination losses, helping f-PeSCs maintain their efficiency even at low light levels [151]. A recent study showed that f-PeSCs using SnO_2-fused ETLs achieved PCE of up to 20.6% at 200 lux and 22.6% at 400 lux, demonstrating their effectiveness in converting indoor light into practical energy production [152,153]. These findings highlight the potential of f-PeSCs as sustainable power sources for next-generation indoor electronics, enabling autonomous IoT devices, smart home sensors, and wearable health monitoring systems.

5.5. Tandem and Hybrid Designs for Enhanced Indoor Performance

To further enhance the efficiency and versatility of f-PeSCs in indoor environments, single-cell functions, also known as tandems, and hybrid device configurations have been explored, in which perovskite materials are combined with other photovoltaic technologies. Tandem structures are composed of multiple stacked sub-cells with complementary absorption spectra and offer a promising approach to maximize the utilization of ambient light by capturing a wider range of light wavelengths [154]. In particular, perovskite/perovskite tandems exhibited superior performance in indoor lighting conditions, with PCE on the order of 26.4% under reported lux illumination [155]. . These tandem devices consist of two perovskite layers with different band gaps, one optimized for the absorption of blue-green light, while the second is optimized to absorb light in the red-near-infrared wavelength range, enabling more efficient photon harvesting across the entire visible spectrum [156]. Researchers have reported the successful creation of long-lasting tandem f-PeSCs that retain more than 90% of their initial single-cell efficiency after 1000 hours of operation in ambient light [157]. Hybrid configurations, which combine perovskite materials with organic photovoltaics (OPV), have also shown significant potential for indoor applications. These f-PeSCs/OPV hybrids combine the efficiency of perovskites with the flexibility and low-cost processing benefits of organic semiconductors, promising to make them well-suited for powering wearable electronics, IoT sensors, and smart home devices [158]. Studies have demonstrated that perovskite/organic hybrid cells can achieve PCEs of >40% under 1000 lux illumination, surpassing the performance of standalone f-PeSCs and OPVs in indoor settings [159]. In 2023, it was reported that the efficiency of f-PeSCs under artificial light (indoors) differs from that under sunlight (outdoors), with a much narrower spectrum, primarily visible, and a typical intensity factor of 500 to 1,000 times lower. That attained a PCE of 39.9-42.4% under 100-1000 lux, maintaining stable performance over 1000 hours of continuous indoor light exposure [160,161]. This stability was attributed to the suppression of ion migration and interfacial degradation through optimized charge transport layers and encapsulation strategies [162]. Additionally, bifacial hybrid f-PeSCs incorporating carbon nanotube (CNT) electrodes have demonstrated enhanced light capture from both front and rear sides, achieving PCEs of up to 27.1% [163]. These advancements highlight the potential of tandem and hybrid designs to push the limits of indoor solar energy harvesting, enabling ultra-efficient and durable f-PeSCs for next-generation low-power electronics [164].

View Article Online
DOI: 10.1039/D5YA00363F

5.6. Material Optimization Strategies for Enhancing f-PeSCs Performance

Material optimization plays a crucial role in improving the efficiency and stability of f-PeSCs, particularly in challenging indoor and outdoor environments. One of the key strategies involves tailoring the composition of perovskite materials to achieve optimal optoelectronic properties. Mixed-halide perovskites, such as $MAPb(I_{1-x}Br_x)_3$, have been extensively studied for their ability to fine-tune the bandgap, allowing f-PeSCs to better match the spectral distribution of indoor lighting sources like LEDs and fluorescent lamps [165]. Research has shown that adjusting the bromine content in these perovskites can shift the absorption edge towards the visible spectrum, enhancing photon utilization and PCE under low-light conditions [166]. Additionally, chlorine-doped perovskites have demonstrated improved crystallinity and reduced defect density, leading to higher carrier mobility and longer charge diffusion lengths, which are essential for maintaining high efficiency in flexible solar cells [167]. Metal halide perovskites, characterized by the general formula ABX_3 (**Figure 15a**) represents an organic or inorganic monovalent cation (e.g., $CH_3NH_3^+$, $CH(NH_2)_2^+$, Cs^+), B denotes a metal cation (e.g., Pb^{2+}), and X signifies a halide anion (Cl^-, Br^-, or I^-), have garnered significant attention due to their exceptional optoelectronic properties. These properties include defect tolerance, a tunable direct bandgap, extended carrier diffusion lengths, high carrier mobility, and compatibility with cost-effective solution- or vapor-based fabrication techniques [168–173]. In addition to their success in photovoltaic applications, perovskites have emerged as promising candidates for next-generation light-emitting devices. Notably, perovskite light-emitting diodes (PeLEDs) exhibit outstanding emission quality, characterized by narrow linewidths, precisely tunable colors, and highly efficient electroluminescence (EL), as depicted in **Figure 15b–e**.

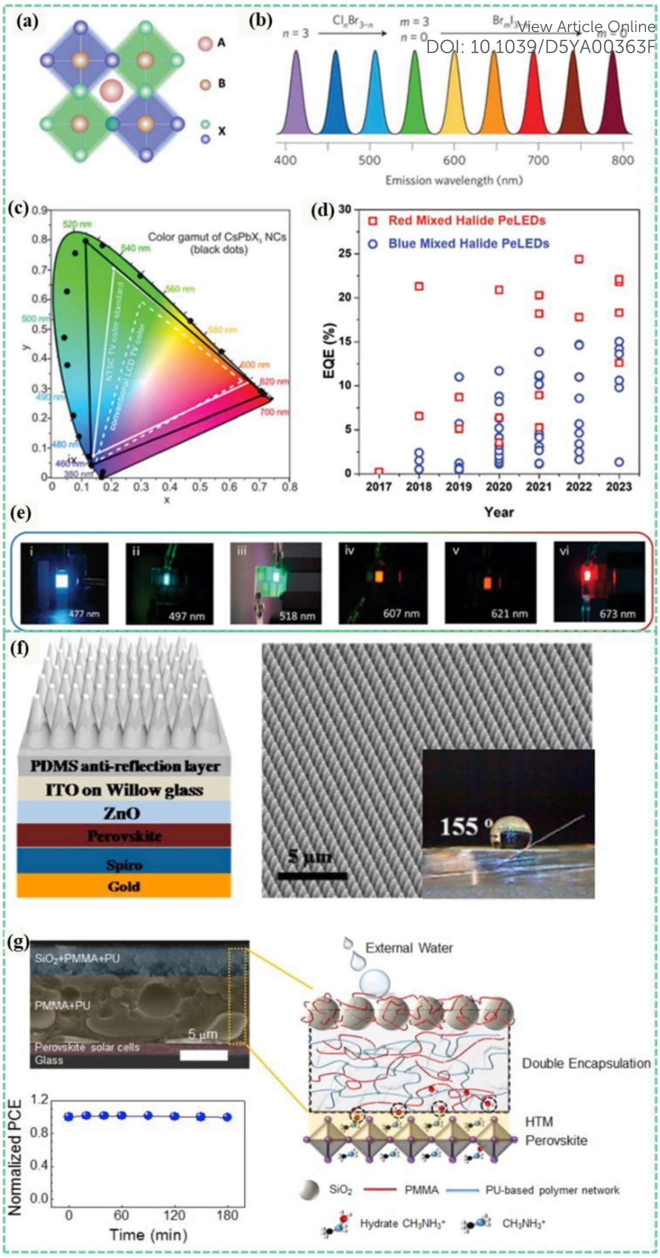

Figure 15. Schematic and performance overview of mixed halide perovskite emitters for full-color electroluminescence: (**a**) Crystal structure of mixed halide perovskites. (**b**) Tunable emission spectra of $CH_3NH_3PbX_{□}Y_{3-□}$ (X,Y = Cl, Br, or I). (**c**) CIE color coordinates and color gamut of perovskite nanocrystals compared to LCD and NTSC TV standards. (**d**) Summary of peak external quantum efficiencies (EQEs) of state-of-the-art mixed halide PeLEDs (**e**) Photographs of operational mixed halide PeLEDs emitting colors from blue to red. (i–vi). Reproduced with permission (License CC BY-NC-ND) from Ref. [174], Copyright (2024), Wiley. Water-Resistant Strategies for Perovskite Solar Cells in Humid Conditions: (**f**) PSC device with nanocone PDMS

View Article Online
DOI: 10.1039/D5YA00363F

layer exhibiting antireflective and superhydrophobic properties (contact angle ~155°). SEM shows PDMS nanocone structure. (**g**) Cross-sectional SEM of PMMA-PU-SiO_2–PMMA-PU double-layer encapsulation. Reproduced with permission from Ref. [175], Copyright (2019), Elsevier.

Beyond compositional tuning, the incorporation of surfactants and passivation agents has proven effective in enhancing film quality and mitigating degradation pathways. Long-chain phospholipid (LP) surfactants have been utilized to promote uniform perovskite crystallization, resulting in smoother and more defect-free films that exhibit improved charge transport characteristics [176,177]. Surface passivation using self-assembled monolayers (SAMs) and poly(3,4-ethylenedioxythiophene):polystyrene sulfonate (PEDOT:PSS) has further contributed to reducing non-radiative recombination losses, thereby boosting overall device efficiency [178]. Studies have demonstrated that f-PeSCs employing SAM-modified interfaces can maintain over 95% of their initial PCE after 2000 hours of indoor operation, highlighting the effectiveness of these strategies in enhancing long-term stability [179,180]. Additionally, hole transport layer (HTL) engineering using materials such as poly(3-hexylthiophene) (P3HT) and copper thiocyanate (CuSCN) has led to improved charge extraction and reduced series resistance, contributing to higher fill factors and overall efficiency improvements [181]. Electrode materials also play a vital role in f-PeSCs performance, particularly in ensuring mechanical durability and electrical conductivity. Transparent conductive oxides (TCOs) such as indium tin oxide (ITO) and fluorine-doped tin oxide (FTO) are commonly used in rigid perovskite solar cells; however, their brittleness makes them unsuitable for flexible applications [175]. Alternative electrode materials, including silver nanowires, graphene, and carbon-based composites, have gained attention for their excellent mechanical flexibility and optical transparency [182]. Carbon electrodes, in particular, offer advantages in terms of cost-effectiveness, chemical stability, and ease of large-scale fabrication, making them a promising candidate for scalable f-PeSCs production [183]. Research has shown that f-PeSCs utilizing carbon electrodes can retain up to 92% of their initial efficiency after 3000 hours of operation under indoor lighting conditions, demonstrating their potential for long-term reliability in real-world applications [184]. These material optimization strategies collectively contribute to enhancing f-PeSCs performance, addressing key challenges related to efficiency, stability, and manufacturability in both indoor and outdoor environments.

5.7. Encapsulation Techniques for Enhancing Environmental Stability of f-PeSCs

Encapsulation is a critical strategy for improving the environmental stability of f-PeSCs, particularly against moisture and oxygen-induced degradation. Since perovskite materials are highly susceptible to hydrolysis and oxidative decomposition, effective encapsulation methods are essential for prolonging device lifetimes in both indoor and outdoor applications. Various encapsulation techniques, including barrier films, laminated coatings, and hybrid encapsulation schemes, have been developed to provide multi-layer protection against external environmental stresses [185]. Barrier films composed of inorganic materials such as aluminum oxide (Al_2O_3), silicon nitride (Si_3N_4), and silicon dioxide (SiO_2) have been extensively studied for their ability to block moisture permeation at the molecular level [186,187]. Atomic layer deposition (ALD) and plasma-enhanced chemical vapor deposition (PECVD) techniques have been employed to fabricate ultra-thin, high-density barrier layers that minimize water vapor transmission rates (WVTR) below 10^{-3} g/(m²·day), significantly enhancing f-PeSCs longevity [188,189]. Laminated coatings, often based on thermoplastic polymers such as ethylene vinyl acetate (EVA) and polyvinyl butyral (PVB), offer an additional layer of mechanical protection while acting as secondary moisture barriers [190]. These coatings are particularly beneficial for large-scale f-PeSCs modules intended for BIPV and VIPV, where physical durability and environmental resistance are paramount [191]. To enhance both optical performance and environmental resistance, functional encapsulation materials with distinct properties have been incorporated. A nanocone-structured PDMS layer, applied to the front of the flexible substrate, provides dual benefits: it enhances optical transmittance due to its antireflective surface and exhibits strong water-repelling characteristics as shown in **Figure 15f**. A multilayer encapsulation system composed of hydrophobic and hydrophilic components has proven effective in protecting perovskite solar cells (PSCs) under highly humid conditions. The outer hydrophobic layer, made of a composite film containing poly(methyl methacrylate) (PMMA), polyurethane (PU), and SiO_2 nanoparticles, acts as a barrier against moisture ingress, as illustrated in **Figure 15g**. Beneath this, a more hydrophilic PMMA layer functions

View Article Online
DOI: 10.1039/D5YA00363F

as an internal desiccant, absorbing residual moisture from the perovskite during device operation. Hybrid encapsulation strategies combining both inorganic and organic layers have demonstrated superior performance in mitigating degradation pathways. One notable approach involves the use of multilayer stacks comprising alternating inorganic and organic films, such as Al_2O_3/polymer/Al_2O_3, which provide both high moisture resistance and mechanical flexibility [192]. The barrier properties of PDMS/Al_2O_3 hybrid films were evaluated using 8×8 Ca arrays encapsulated with different film structures, as shown in **Figure 16a**. After 12 h under 25 °C/50% RH conditions, samples with Al_2O_3/PDMS showed full oxidation, whereas those with PDMS/Al_2O_3 retained partial stability **Figure 16b**, reflected in higher survival ratios (S/S_0) in **Figure 19c**. This highlights the superior barrier performance of the PDMS-first configuration, where Al_2O_3 fills PDMS pores during deposition. Encapsulation efficiency improved with increased precursor pulse time up to a point, after which performance declined due to saturation effects governed by ALD molecular dynamics. Temperature also played a role: films prepared at 90 °C with 1 s TMA pulse showed the best results **Figure 16d** and **Figure 16e**. These findings support the use of PDMS/Al_2O_3 hybrid films for effective moisture protection, especially under temperature-sensitive device conditions as shown **Figure 16f-h**. These hybrid structures effectively suppress water vapor penetration while accommodating bending-induced stress, ensuring long-term operational stability even under dynamic outdoor conditions [193]. Another emerging encapsulation technique involves the incorporation of desiccant materials, such as calcium oxide (CaO) and molecular sieves, within the encapsulation layer to actively scavenge residual moisture within the device package [194]. Studies have shown that integrating desiccants into f-PeSCs encapsulation can extend operational lifespans beyond 1000 hours under accelerated aging tests at 85°C and 85% relative humidity (RH), making them viable for commercial applications requiring prolonged environmental resilience [195]. Additionally, recent advancements in UV-resistant encapsulants, such as fluorinated polymers and UV-absorbing resins, have further enhanced f-PeSCs durability by protecting the perovskite layer from photodegradation caused by prolonged exposure to ultraviolet radiation [196–198]. These encapsulation innovations collectively contribute to overcoming the environmental stability challenges faced by f-PeSCs, paving the way for their integration into durable and commercially viable solar technologies.

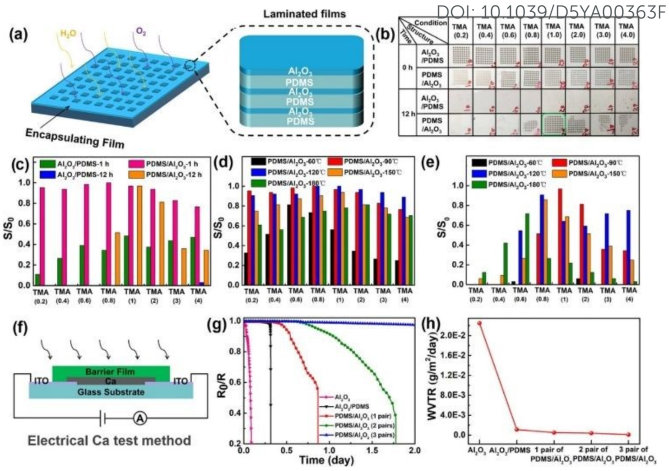

Figure 16. (**a**) Schematic of Ca arrays encapsulated with laminated films. (b) Corrosion evolution and (**c**) survival ratio statistics after 12 h. (**d**, **e**) Survival ratios of Ca arrays with PDMS/Al_2O_3 films at varying temperatures after 1 h and 12 h. (**f**) Electrical test setup. (**g**) Normalized conductance over time at 25 °C/50% RH. (**h**) WVTR comparison for different film structures. Reproduced with permission from Ref. [192], Copyright (2023), American Chemical Society.

5.8. Prospects and Challenges for f-PeSCs Commercialization

The rapid advancements in f-PeSCs have positioned them as a compelling alternative to conventional photovoltaic technologies, particularly for applications requiring lightweight, bendable, and adaptable energy solutions. Their superior performance in both indoor and outdoor environments, coupled with the potential for scalable manufacturing, has fueled extensive research aimed at overcoming existing limitations and accelerating commercialization. Despite the significant progress made in enhancing efficiency, stability, and mechanical durability, several challenges remain before f-PeSCs can achieve widespread market adoption. Foremost among these is the need for long-term environmental stability, particularly in humid and high-temperature conditions, which continues to be a major bottleneck for outdoor applications. Although encapsulation techniques and material modifications have demonstrated promising results in mitigating degradation, further refinements are necessary to meet industry-standard lifespans of 15–20 years for photovoltaic modules [199]. Additionally, the mechanical reliability of f-PeSCs under continuous bending and flexing remains a concern, especially for applications involving wearable electronics and

View Article Online
DOI: 10.1039/D5YA00363F

foldable solar panels, necessitating continued innovation in substrate materials and self-healing technologies [200].

From a manufacturing perspective, while scalable fabrication techniques such as R2R printing, slot-die coating, and inkjet printing have shown potential for large-area f-PeSCs production, achieving consistent film quality and high throughput at competitive costs remains a challenge. The transition from laboratory-scale devices to industrial-scale modules requires stringent process control and optimization of deposition techniques to ensure uniform perovskite layers free from defects [201]. Furthermore, the integration of f-PeSCs into existing energy systems and building infrastructures demands compatibility with current photovoltaic standards and regulations, which may necessitate adjustments in module design and certification protocols [202]. On the economic front, the cost-effectiveness of f-PeSCs hinges on the availability of affordable, high-performance materials and the development of cost-efficient manufacturing processes. While some studies suggest that f-PeSCs could potentially undercut the production costs of rigid perovskite solar cells and silicon-based modules within the next decade, realizing this vision will depend on sustained investment in research, technological innovation, and industrial partnerships [203]. Looking ahead, the convergence of f-PeSCs technology with emerging fields such as energy storage, smart architecture, and AI-assisted design holds immense potential for expanding their applications beyond traditional solar power generation. The integration of f-PeSCs with flexible energy storage systems, semi-transparent smart windows, and biodegradable materials underscores their versatility in addressing diverse energy needs across multiple sectors[204]. Moreover, the application of machine learning and computational modeling in optimizing perovskite compositions and device architectures is expected to accelerate the discovery of novel materials and fabrication strategies, further enhancing f-PeSCs performance and durability [205]. As research efforts continue to refine these aspects, f-PeSCs are poised to play a pivotal role in shaping the future of renewable energy, smart electronics, and sustainable infrastructure, provided that ongoing challenges in stability, scalability, and commercial viability are effectively addressed [206,207].

5.9. Flexible-Perovskite Solar Cells Aligned with SDGs

The unique attributes of flexible Perovskite solar cells (f-PeSCs), their potential for low-cost manufacturing, lightweight and conformable nature, and improving performance metrics-position them as a significant technological catalyst for achieving several SDGs as shown in **Table 4**. This section explores how perovskite Solar Cells contribute the advancement of SDGs especially, Goal 7(Affordable and clean energy), 9 (industry, innovations and infrastructure), 11 (Sustainable cities and communities), 12 (Sustainable production and consumption), 13 (Climate action) and 17 (partnerships for the goals)

Table 4. Matrix of the main contributions of f-PeSCs to the SDGs

SDG Target	Key Attribute/Application of f-PeSCs	Supporting Evidence	Ref.
SDG 7	Lower EPBT, potential for low LCOE, suitability for off-grid/decentralized power, lightweight for diverse deployment.	(Baraneedharan et al., 2024)	208
SDG 9	R2R manufacturing innovation, enabling BIPV, VIPV, IoT power; fostering new materials science and industrial ecosystems.	(Brian, 2025)	209
SDG 11	BIPV for smart, energy-producing buildings and urban design; decentralized urban energy systems; lightweight for retrofitting existing structures.	(Jung-Kun Lee, 2023)	210
SDG 12	Development of lead-free alternatives, advanced recycling processes (water-based, closed-loop), lower material intensity, and design for sustainability.	(Booten et al., 2021)	211
SDG 13	Significantly lower GHG emissions and carbon footprint during manufacturing compared to silicon PV.	(McCalmont et al., 2023)	212
SDG 17	Driven by international R&D collaborations, public-private partnerships, and substantial government funding initiatives globally.	(Leccisi & Fthenakis, 2021)	213

5.9.1. SDG7 - Enhancing energy access, cost-competitiveness, and energy and payback time

The f-PeSCs offer a compelling pathway to advance SDG7 by making clean energy more affordable and accessible. In terms of affordability and cost-competitiveness, the potential for lower manufacturing costs is a primary driver. Solution processability, particularly through record to report (R2R) techniques, promises reduced capital expenditure for factories and higher throught compared to conventional silicon PV manufacturing [208]. Material usage can also be lower, techno-economic analyses project R2R perovskite solar film costs to be as low as \$0.04-\$0.10 per watt at gigawatt-scale production [214]. However, efficient recycling processes are projected to significantly reduce the levelized cost of electricity (LCOE) by recovering valuable material. In clean energy and energy access, the versatility of f-PeSCs stemming from their lightweight and conformable where traditional heavy, rigid panels are impractical or

View Article Online
DOI: 10.1039/D5YA00363F

too costly to transport and install. This is particularly relevant for developing countries and for applications like portable power for disaster relief or mobile charging solutions [215]. In energy payback time (EPBT), f-PeSCs, in general, exhibit a significantly shorter EPBT compared to silicon PV. Several studies indicate an EPBT of around 0.35 years for all-perovskite tandem configurations, compared to 1.52 years for a silicon benchmark. The flexible form factor itself can contribute to an additional 6% improvement in EPBT, likely due to reduced material and energy inputs in manufacturing and transportation. A shorter EPBT means that the solar cell repays the energy invested in its production much faster, leading to a quicker net energy gain [216]. The confluence of potentially lower manufacturing costs, a dramatically shorter EPBT, and suitability for decentralized applications positions f-PeSCs as a technology uniquely aligned with the affordable and accessible all dimensions of SDG7. This is especially true for resource-constrained environments or for niche applications where conventional solar solutions or standard rooftop installations, f-PeSCs can empower communities and individuals stability comparable to silicon; frequent replacements due to premature degradation would negate the initial cost advantages and inflate the LCOE.

5.9.2. SDG 9 - Driving innovation in materials, advanced manufacturing, and enabling novel infrastructures.

The f-PeSCs are a nexus of innovation, driving advancements in materials science, manufacturing technologies, and the very concept of energy-generating infrastructure. Innovation in materials science, the field of f-PeSCs research is exceptionally dynamic, characterized by continuous exploration of new perovskite compositions, interfacial layers, charge transport materials, additives for stability and efficiency enhancement, and crucially, lead-free alternatives. This relentless innovation contributes directly to the knowledge base underpinning advanced materials. In advanced manufacturing, the development and scaling of R2R printing and other high-throughput solution-based processing techniques for f-PeSCs represent a significant leap in photovoltaic manufacturing technology [217]. This not only promises lower costs but also fosters a new industrial ecosystem around advanced coating, printing, and materials handling. The

novel infrastructures, the unique factor of f-PeSCs, enables their integration into structures and devices in ways previously unimaginable. In the case of building-integrated photovoltaic (BIPV), f-PeSCs can be seamlessly incorporated into curved facades, windows (semi-transparent variants), roofing materials, and building fabrics, transforming static building envelopes into active energy generators. Panasonic's demonstration of BIPV perovskite glass is a case in point [218]. In the vehicle-integrated photovoltaic (VIPV), their lightweight and conformable nature makes f-PeSCs suitable for application on vehicle roofs, bodies, or even sails (for marine applications), potentially extending the range of electric vehicles or powering auxiliary systems. In this case, powering IoT devices, f-PeSCs can provide autonomous power for the burgeoning number of IoT sensors and devices, reducing reliance on batteries and enabling widespread deployment in smart infrastructure. The f-PeSCs are thus more than an incremental improvement; they serve as an enabling platform for a new generation of smart and energy-harvesting infrastructure. This fosters industrial diversification, creates demand for high-tech manufacturing, and contributes to more resilient and distributed energy systems. The innovation spurred by f-PeSCs extends across the entire value chain, from raw material synthesis and precursor formulation to manufacturing equipment design and end-product integration technologies. Investment in R&D for f-PeSCs manufacturing, such as the EU's Horizon Europe LUMINOSITY and PEARL projects, directly stimulates this industrial innovation and the development of novel infrastructure capabilities. For widespread adoption in BIPV and VIPV, the development of industry-specific standards for performance, durability, and integration protocols will be crucial, necessitating collaboration between f-PeSCs manufacturers, the construction industry, and automotive companies.

5.9.3. SDG 11 - Contributions to smart urban development. Building-integrated solutions and decentralized energy systems.

The attributes of f-PeSCs align well with the goals of creating sustainable, resilient, and inclusive urban environments. f-PeSCs can be integrated into various elements of the smart urban development, such as bus shelters, noise barriers, public lighting, and even pavements or facades of public transport infrastructure. This contributes to energy-efficient urban design and can enhance the aesthetic appeal of cities by offering less obtrusive renewable energy solutions. In building-integrated solutions as highlighted under SDG 9, BIPV is a key application where f-PeSCs can transform buildings from passive energy consumers into active producers. Their

View Article Online
DOI: 10.1039/D5YA00363F

lightweight nature is particularly advantageous for retrofitting existing buildings that may not have the structural capacity for heavy conventional solar panels [219]. The f-PeSCs facilitate localized power generation at the point of use, thus decentralizing energy systems. This reduces reliance on centralized electricity grids, minimizes transmission losses, and can enhance urban energy resilience, especially when coupled with local energy storage solutions. In the event of grid outages, buildings or communities with integrated f-PeSCs could maintain power for essential services. The F-PeSCs offer the potential to fundamentally alter the urban energy landscape and aesthetic. By enabling nearly any sun-exposed surface to become a power generator, they allow for a more organic and less visually intrusive integration of renewable energy compared to traditional, often bulky, silicon panels. This capability to weave energy generation into the architectural design of cities supports the creation of more sustainable and visually harmonious urban spaces. The success of BIPS applications, however, is heavily contingent on overcoming the mechanical and long-term environmental stability challenges to ensure these integrated systems meet stringent building codes and match the expected lifetimes of building components [220]. Consequently, urban planning policies and building regulations will need to evolve to actively incorporate and incentivize the use of innovative BIPS solutions like f-PeSCs, addressing aspects such as fire safety, durability standards, aesthetic guidelines, and end-of-life management protocols.

5.9.4. SDG12 - Life cycle impacts, strategies for lead mitigation, recycling, and fostering a circular economy for f-PeSCs

Achieving sustainable energy solutions necessitates a strong focus on responsible consumption and production patterns, an area where F-PeSCs present both challenges and significant opportunities. Generally, F-PeSCs exhibit lower embodied energy and manufacturing-related greenhouse gas emissions compared to conventional silicon PV, primarily due to lower processing temperatures and potentially less material-intensive fabrication. For instance, one study indicated that an alternative low-dimensional f-PeSCs configuration had lower average environmental impacts than reference f-PeSCs. Solvent usage during manufacturing has been identified as a key variable in LCA results; the use of recycled organic solvents can lead to a substantial reduction in global warming potential (GWP)-over 26% in some systems [213]. The presence of lead in many of the highest-performing f-PeSCs formulations is a primary environmental and health concern, potentially hindering their widespread adoption and posing risks if not managed responsibly. Several strategies are being pursued to address this reducing lead content, alloying lead with other metals, or using mixed halide perovskite compositions can reduce the overall lead percentage. Intensive research is focused on replacing lead entirely with less toxic elements like tin, germanium, bismuth, or antimony, or by developing a double perovskite structure [221]. Others have been the robust encapsulation aims to prevent lead leakage during the operational life of the cell. Innovative lead sequestration layers are being developed to chemically bind any lead that might escape, preventing its release into the environment. Recycling and circular economy of f-PeSCs, particularly those made via solution processing, offer high potential for material recovery and recycling [212]. Economically feasible recycling processes have been developed that can recover valuable materials such as lead, silver, gold, glass, and ITO from waste f-PeSCs. The net cost of recycling can even be negative, indicating a potential economic benefit. The challenge posed by toxicity has, somewhat paradoxically, spurred remarkable innovation in material science (eg., lead-free perovskites) and green chemistry, engineering. This proactive approach clouds the position f-PeSCs as a model for sustainable material design and end-of-life management within the broader electronics sector. The economic viability of this recycling process is a powerful driver for their adoption, transforming a potential environmental liability into an economic opportunity and reinforcing circular economy principles. For f-PeSCs specifically, the focus must extend to the recyclability of not only the active but also the flexible substrates (often polymers) and encapsulation materials, an area that requires further dedicated research to achieve true circularity.

5.9.5. SDG 13 - Potential for greenhouse gas emission reduction and lower carbon footprint compared to incumbent technologies.

The deployment of f-PeSCs can make a substantial contribution to climate change mitigation efforts due to their favorable carbon footprint characteristics; Lower greenhouse gas emission factor: Life cycle analyses indicate that all-perovskite tandem solar Cells can have a GHG emission factor as low as 10.7 g CO_2 eq/kWh. This is significantly lower than that of conventional silicon PV (around 24.6g $CO_{2\,eq}$ /kWh) and even perovskite-silicon tandem cells(around 46.38g

View Article Online
DOI: 10.1039/D5YA00363F

$CO_{2\ eq}$/kWh) due to the energy-intensive silicon component [216]. The research indicates that the carbon footprint associated with the manufacturing of perovskite PVs is estimated to be 40-60% lower than that of silicon PV. This advantage stems from lower energy requirements during production. The flexible nature of f-PeSCs can further reduce GHG emissions by approximately 6% compared to their rigid counterparts. This is likely due to reduced material consumption (thinner layer, lighter substrates), lower transportation emissions, and potentially less energy-intensive manufacturing processes like R2R. Photovoltaic, as a whole, is already making a significant contribution to reducing global GHG emissions, with an estimated 0.92 gigatons of CO_2 avoided in 2023, representing about 2.5% of all energy sector emissions. The adoption of lower-carbon f-PeSCs technology can amplify this positive impact [219]. The significantly lower carbon footprint and shorter energy payback time of f-PeSCs, particularly flexible and all-perovskite tandem configurations, imply that a transition towards f-PeSCs dominant solar energy could accelerate decarbonizing efforts more rapidly per unit of energy produced compared to relying solely on established silicon PV technology. For every kilowatt-hour generated, the embedded carbon from the manufacturing phases is substantially less for f-PeSCs. If f-PeSCs can achieve operational lifetimes and efficiencies comparable to silicon in real-world conditions, their overall life-cycle emissions will be considerably lower, making them a more potent tool for climate mitigation. However, this potential is heavily dependent on achieving a long operational lifetime, premature degradation and replacement would increase the cumulative carbon footprint, diminishing this key advantage. Global and national climate policies should, therefore, consider the lifecycle GHG benefits of emerging PV technologies like F-PeSCs when designing incentives and deployment strategies, potentially fast-tracking their adoption where appropriate.

5.9.6. SDG 17 - international collaborations, public-private partnerships, and government/supranational funding in advancing f-PeSCs technology.

The rapid progress and future trajectory of f-PeSCs technology are intrinsically linked to robust partnerships across academia, industry, and government, both nationally and internationally. The development of f-PeSCs is a global endeavor, with numerous examples of fruitful international research collaborations. These include the CSIRO-led international team achieving the CPMAC molecule for enhanced stability and efficiency, and the collaboration between Linköping University (Sweden) and Cornell University (USA) on water-based recycling methods. Such collaborations pool diverse expertise and resources, accelerating discovery. Government and super national funding; governments like US department of energy (DOE) and its national renewable energy laboratory (NREL) have provided significant funding trough program [222], the horizon Europe framework program is funding key projects like Luminosity and pearl which focus advancing manufacturing of f-PeSCs and exploring perovskite integration of fabrics for achieving efficiency, cost, stability, and environmental footprint. Academia-Industry partnerships: The synergy between HEI-industries is vital for translating laboratory discoveries into commercially viable products and processes. For instance, Oxford PV, a spin-out from the University of Oxford, is commercializing perovskite-silicon tandem cells [223]. The rapid advancement of f-PeSCs technology, especially its flexible variants, is a clear testament to the efficacy of global research. International collaborations accelerate the pace of discovery by pooling diverse talent and resources, and market-ready products. This collaborative model is essential for tracking complex global challenges like the transition to sustainable energy. Strong intellectual property frameworks and transparent mechanisms for international R&D collaboration, such as the patent licensing agreement between Oxford PV and Trinasolar, are vital for sustaining this innovation pipeline and facilitating technology transfer. Continued and enhanced international cooperation on pre-competitive research, the development of harmonized standards (e.g, for stability testing and performance rating of f-PeSCs), and the promotion of sustainable manufacturing practice will be key to unlocking the full global potential of f-PeSCs technology.

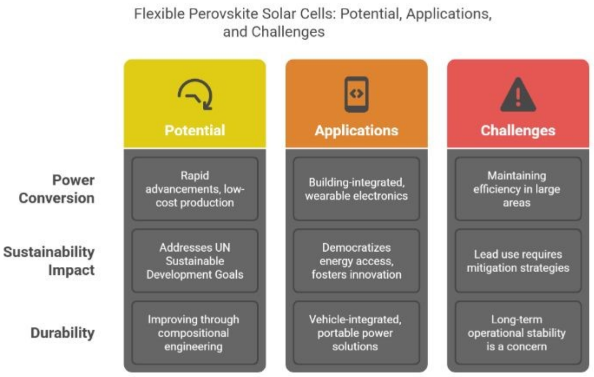

Flexible Perovskite Solar Cells: Potential, Applications, and Challenges

	Potential	Applications	Challenges
Power Conversion	Rapid advancements, low-cost production	Building-integrated, wearable electronics	Maintaining efficiency in large areas
Sustainability Impact	Addresses UN Sustainable Development Goals	Democratizes energy access, fosters innovation	Lead use requires mitigation strategies
Durability	Improving through compositional engineering	Vehicle-integrated, portable power solutions	Long-term operational stability is a concern

Figure 17. Potential, Applications, and Challenges of PCSs

View Article Online
DOI: 10.1039/D5YA00363F

Flexible perovskite Solar Cells stand at a pivotal juncture **(Figure 17)**, offering a compelling convergence of advanced materials science, innovative manufacturing potential, and a unique to address pressing global sustainability challenges. This review has underscored the significant potential of f-PeSCs to act as a catalyst in achieving key UN Sustainable Development Goals, particularly those related to affordable and clean energy (SDG 7), industry, innovation, and infrastructure (SDG9), sustainable cities and communities (SDG 11), responsible consumption and production (SDG 12), climate action (SDG 13), and partnerships for the goals (SDG 17). The journey of f-PeSCs is characterized by rapid advancements in PCE and the promise of low–cost production, largely driven by their solution processability and amenability to high through techniques like R2R manufacturing. Their inherent flexibility, lightweight, and conformability unlock a spectrum of novel applications, ranging from building-integrated and vehicle-integrated photovoltaics to wearable electronics and portable power solutions, which are often beyond the reach of conventional rigid solar technologies. These applications can democratise access to energy, foster industrial innovation, create more innovative and more resilient urban environments, and contribute to a low-carbon future.

5.9.7. Recycling Challenges of f-PeSCs

Despite promising performance, recycling and end-of-life management remain critical challenges for flexible perovskite solar cells [224,225]. The presence of lead-based perovskite compounds raises environmental concerns in cases of improper disposal. Several strategies have been proposed to mitigate this problem, including lead encapsulation, solvent extraction recovery processes, and the development of lead-free alternatives based on tin, germanium, or bismuth [226]. Furthermore, flexible substrates such as PET and PEN can hinder recycling due to the multilayer nature of the devices [227,228]. Future research should focus on circular design strategies, encompassing material recovery processes, recyclable substrates, and environmentally benign perovskite compositions, aiming to ensure the sustainable implementation of flexible photovoltaic technologies.

6. Emerging Trends & Future Prospects

Flexible perovskite solar cells are advancing toward broader commercialization and diverse applications through several emerging trends. A key development is their integration with energy storage systems, such as flexible supercapacitors and thin-film batteries, enabling self-sustaining power solutions for portable electronics, smart textiles, and IoT devices. These lightweight, bendable systems support efficient energy harvesting, storage, and real-time use, making them ideal for wearable health monitors, e-textiles, and autonomous sensors that operate without external charging. Advances in printed battery technologies, such as flexible lithium-ion and solid-state batteries, further enhance compatibility, opening up possibilities for compact, self-powered electronics. Another promising direction is the development of semi-transparent f-PeSCs for smart windows, which serve as both power generators and aesthetic architectural elements. By tailoring the bandgaps of perovskite cells, these devices allow for selective visible light transmission while absorbing near-infrared wavelengths for energy conversion, thereby supporting energy-efficient smart cities and net-zero energy buildings without compromising natural lighting. Recent studies have shown that semi-transparent f-PeSCs can achieve high power conversion efficiencies under indoor illumination, with significant visible transmittance, bolstered by innovations in transparent conductive materials such as silver nanowires, graphene, and metal mesh electrodes, which align with existing window manufacturing processes. Sustainability is also a key focus, with research into bio-inspired and biodegradable f-PeSCs aimed at addressing environmental concerns. Eco-friendly alternatives, including cellulose-based substrates, biodegradable encapsulation layers, and non-toxic perovskite formulations like tin- and bismuth-based compositions, aim to minimize hazardous waste. While lead-free perovskites currently exhibit lower efficiency, efforts in compositional engineering and interface optimization aim to enhance their optoelectronic properties, aligning with global sustainability goals. Additionally, machine learning and AI-driven methodologies are accelerating the development of f-PeSCs by optimizing perovskite compositions, device architectures, and fabrication parameters. These approaches analyze extensive experimental datasets to identify high-performance materials and simulate degradation mechanisms, enhancing device stability and efficiency. AI-driven breakthroughs in hole transport materials and electron transport layers are reducing development cycles, expediting the path to commercialization. Together, these

View Article Online
DOI: 10.1039/D5YA00363F

interdisciplinary advancements in materials science, energy storage, sustainable design, and computational innovation position f-PeSCs as a transformative force in renewable energy, smart architecture, and autonomous electronics, with significant potential to shape the global clean energy landscape.

7. Conclusion

Flexible perovskite solar cells have emerged as a cornerstone of next-generation photovoltaic technologies, demonstrating remarkable progress in efficiency, flexibility, and applicability across diverse environments. This review highlights the significant progress of f-PeSCs from 2012 to 2024, achieving power conversion efficiencies of up to 41% under indoor lighting conditions and demonstrating notable improvements in mechanical durability and environmental stability. Innovations in low-temperature processing, scalable manufacturing techniques like R2R printing, and sustainable material strategies, including lead-free perovskites and recyclable substrates, position f-PeSCs as a viable solution for applications ranging from wearable electronics to building-integrated photovoltaics. However, challenges such as long-term stability under outdoor conditions, scalability for large-area production, and environmental concerns related to lead toxicity necessitate continued research and innovation. The integration of AI-driven material design, advanced encapsulation techniques, and bio-inspired substrates offers promising avenues to overcome these hurdles. Aligning with key SDGs, especially in affordable clean energy, industrial innovation, and climate action, f-PeSCs have the potential to transform the global energy landscape significantly. Ongoing interdisciplinary collaboration and investment in sustainable manufacturing will be essential to achieving their commercial viability and ensuring they catalyze a sustainable, low-carbon future.

Competing Interests

The authors declare no relevant financial or non-financial interests.

Author Contribution Statement

Thiago F. Santos, PhD Student (Conceptualization: Lead; Methodology: Equal; Validation: Lead; Writing – original draft: Lead). ***Caroliny C. Santos***, PhD Student (Conceptualization: Lead; Methodology: Supporting; Validation: Lead; Writing – original draft: Lead). ***Vishnu Vijay Kumar*** (Writing – original draft: Equal). ***Bahati Shabani Nzeyimana*** (Writing – original draft: Equal; Writing – review & editing: Equal). ***H Jeevan Rao*** (Writing – original draft: Equal). ***Bhargav Akkinepally*** (Writing – original draft: Equal; Writing – review & editing: Equal). ***Domingos F. S. Souza*** (Investigation: Equal; Methodology: Equal). ***Jose H. O. Nascimento*** (Funding acquisition: Lead; Project administration: Lead; Resources: Lead; Validation: Equal; Writing – original draft: Equal; Writing – review & editing: Lead).

Acknowledgements

This research was supported by CARREFOUR group and the Coordination for the Improvement of Higher Education Personnel – Brazil (CAPES) – Finance Code 001, as well as to the National Council for Scientific and Technological Development (CNPq) under projects number 400913/2023-2 and 404139/2022-1. Further thanks are due to the Graduate Program in Chemical Engineering at the Federal University of Rio Grande do Norte (PPGEQ/UFRN) for providing technical assistance.

REFERENCES

1 I. E. A. (IEA), *Global electricity demand is set to grow strongly to 2030, underscoring need for investments in grids and flexibility*, .

2 I. E. A. (IEA), *Snapshot of Global PV Markets 2024*, 2024.

3 K. Yoshikawa, W. Yoshida, T. Irie, H. Kawasaki, K. Konishi, H. Ishibashi, T. Asatani, D. Adachi, M. Kanematsu, H. Uzu and K. Yamamoto, *Sol. Energy Mater. Sol. Cells*, 2017, **173**, 37–42.

4 H. Tong, S. Tan, Y. Zhang, Y. He, C. Ding, H. Zhang, J. He, J. Cao, H. Liu, Y. Li, J. Kang, X. Xu, C. Chen, Y. Chen, F. Sun, B. Feng, H. Sun, X. Jiang, L. Yu, J. Li, D. He, J. Li and Z. Li, *Nat. Commun.*, 2025, **16**, 5920.

5 L. A. Castriotta, R. Fuentes Pineda, V. Babu, P. Spinelli, B. Taheri, F. Matteocci, F. Brunetti, K. Wojciechowski and A. Di Carlo, *ACS Appl. Mater. Interfaces*, 2021, **13**, 29576–29584.

6 R. Tian, S. Zhou, Y. Meng, C. Liu and Z. Ge, *Adv. Mater.*, , DOI:10.1002/adma.202311473.

7 S. Kim, H. Van Quy and C. W. Bark, *Mater. Today*

View Article Online
DOI: 10.1039/D5YA00363F

Energy, 2021, **19**, 100583.

8 M. Maoz, Z. Abbas, S. A. B. Shah and V. Lughi, *Sustainability*, 2025, **17**, 1820.

9 T. Jin, W. Li, Y. Li, Y. Luo, Y. Shen, L. Cheng and J. Tang, *Adv. Opt. Mater.*, , DOI:10.1002/adom.201801153.

10 D. Wang, W. Gu, N. Su, F. Liu, Q. Li and B. Du, 2025.

11 Y. Jung, K. Hwang, Y. Heo, J. Kim, D. Vak and D. Kim, *Adv. Opt. Mater.*, , DOI:10.1002/adom.201701182.

12 A. B. Djurišić, F. Z. Liu, H. W. Tam, M. K. Wong, A. Ng, C. Surya, W. Chen and Z. B. He, *Prog. Quantum Electron.*, 2017, **53**, 1–37.

13 A. Venkateswararao, J. K. W. Ho, S. K. So, S.-W. Liu and K.-T. Wong, *Mater. Sci. Eng. R Reports*, 2020, **139**, 100517.

14 X. Hou, Y. Wang, H. K. H. Lee, R. Datt, N. Uslar Miano, D. Yan, M. Li, F. Zhu, B. Hou, W. C. Tsoi and Z. Li, *J. Mater. Chem. A*, 2020, **8**, 21503–21525.

15 K.-L. Wang, Y.-H. Zhou, Y.-H. Lou and Z.-K. Wang, *Chem. Sci.*, 2021, **12**, 11936–11954.

16 C. Polyzoidis, K. Rogdakis and E. Kymakis, *Adv. Energy Mater.*, , DOI:10.1002/aenm.202101854.

17 S. Barthwal, R. Kumar and S. Pathak, *ACS Appl. Energy Mater.*, 2022, **5**, 6545–6585.

18 X. Zhu, J. Xu, H. Cen, Z. Wu, H. Dong and J. Xi, *Nanoscale*, 2023, **15**, 5167–5180.

19 L. Zhang, Y. Wang, X. Meng, J. Zhang, P. Wu, M. Wang, F. Cao, C. Chen, Z. Wang, F. Yang, X. Li, Y. Zou, X. Jin, Y. Jiang, H. Li, Y. Liu, T. Bu, B. Yan, Y. Li, J. Fang, L. Xiao, J. Yang, F. Huang, S. Liu, J. Yao, L. Liao, L. Li, F. Zhang, Y. Zhan, Y. Chen, Y. Mai and L. Ding, *Mater. Futur.*, 2024, **3**, 022101.

20 M. Z. Qamar, Z. Khalid, R. Shahid, W. C. Tsoi, Y. K. Mishra, A. K. K. Kyaw and M. A. Saeed, *Nano Energy*, 2024, **129**, 109994.

21 S. B. Kang, P. Patil, G. W. Yoon, G. S. Han, H. S. Jung and D. H. Kim, *Chem. Eng. J.*, 2024, **502**, 157973.

22 P. Kumari, S. Prasanthkumar and L. Giribabu, *Sol. Energy*, 2024, **284**, 113049.

23 T. F. Santos, B. R. Carvalho, E. V. Santos, R. F. P. Pereira, D. F. S. Souza and J. H. O. Nascimento, *Sustain. Energy Fuels*, , DOI:10.1039/D4SE01537A.

24 W. M. Lim, S. Kumar and N. Donthu, *J. Bus. Res.*, 2024, **182**, 114760.

25 N. Donthu, S. Kumar, D. Mukherjee, N. Pandey and W. M. Lim, *J. Bus. Res.*, 2021, **133**, 285–296.

26 M. H. Kumar, N. Yantara, S. Dharani, M. Graetzel, S. Mhaisalkar, P. P. Boix and N. Mathews, *Chem. Commun.*, 2013, **49**, 11089.

27 C. Roldán-Carmona, O. Malinkiewicz, A. Soriano, G. Mínguez Espallargas, A. Garcia, P. Reinecke, T. Kroyer, M. I. Dar, M. K. Nazeeruddin and H. J. Bolink, *Energy Environ. Sci.*, 2014, **7**, 994.

28 S. S. Shin, W. S. Yang, J. H. Noh, J. H. Suk, N. J. Jeon, J. H. Park, J. S. Kim, W. M. Seong and S. Il Seok, *Nat. Commun.*, 2015, **6**, 7410.

29 D. Yang, R. Yang, X. Ren, X. Zhu, Z. Yang, C. Li and S. (Frank) Liu, *Adv. Mater.*, 2016, **28**, 5206–5213.

30 J. Yoon, H. Sung, G. Lee, W. Cho, N. Ahn, H. S. Jung and M. Choi, *Energy Environ. Sci.*, 2017, **10**, 337–345.

31 J. Feng, X. Zhu, Z. Yang, X. Zhang, J. Niu, Z. Wang, S. Zuo, S. Priya, S. (Frank) Liu and D. Yang, *Adv. Mater.*, 2018, **30**, 1801418.

32 K. Huang, Y. Peng, Y. Gao, J. Shi, H. Li, X. Mo, H. Huang, Y. Gao, L. Ding and J. Yang, *Adv. Energy Mater.*, 2019, **9**, 1901419.

33 X. Meng, Z. Cai, Y. Zhang, X. Hu, Z. Xing, Z. Huang, Z. Huang, Y. Cui, T. Hu, M. Su, X. Liao, L. Zhang, F. Wang, Y. Song and Y. Chen, *Nat. Commun.*, 2020, **11**, 3016.

34 S. Wu, Z. Li, J. Zhang, X. Wu, X. Deng, Y. Liu, J. Zhou, C. Zhi, X. Yu, W. C. H. Choy, Z. Zhu and A. K. -Y. Jen, *Adv. Mater.*, , DOI:10.1002/adma.202105539.

35 L. Li, Y. Wang, X. Wang, R. Lin, X. Luo, Z. Liu, K. Zhou, S. Xiong, Q. Bao, G. Chen, Y. Tian, Y. Deng, K. Xiao, J.

View Article Online
DOI: 10.1039/D5YA00363F

Wu, M. I. Saidaminov, H. Lin, C.-Q. Ma, Z. Zhao, Y. Wu, L. Zhang and H. Tan, *Nat. Energy*, 2022, **7**, 708–717.

36 Z. Skafi, J. Xu, V. Mottaghitalab, L. Mivehi, B. Taheri, F. Jafarzadeh, S. K. Podapangi, D. Altamura, M. R. Guascito, L. Barba, C. Giannini, A. Rizzo, F. De Rossi, H. Javanbakht Lomeri, L. Sorbello, F. Matteocci, F. Brunetti and T. M. Brown, *Sol. RRL*, , DOI:10.1002/solr.202300324.

37 C. Liu, T. Yang, W. Cai, Y. Wang, X. Chen, S. Wang, W. Huang, Y. Du, N. Wu, Z. Wang, Y. Yang, J. Feng, T. Niu, Z. Ding and K. Zhao, *Adv. Mater.*, , DOI:10.1002/adma.202311562.

38 E. A. Katz, *Helv. Chim. Acta*, , DOI:10.1002/hlca.202000061.

39 Edmond Becquerel, *Comptes Rendus l'Academie des Sci.*, 1839, **9**, 561–567.

40 A. Einstein, *Am. J. Phys.*, 1905, **33**, 1–16.

41 L. L. Kazmerski, *Sol. Compass*, 2024, **10**, 100073.

42 S. Rahman, A. Haleem, M. Siddiq, M. K. Hussain, S. Qamar, S. Hameed and M. Waris, *RSC Adv.*, 2023, **13**, 19508–19529.

43 M. Liu, M. B. Johnston and H. J. Snaith, *Nature*, 2013, **501**, 395–398.

44 A. Kojima, K. Teshima, Y. Shirai and T. Miyasaka, *J. Am. Chem. Soc.*, 2009, **131**, 6050–6051.

45 J. Jeng, Y. Chiang, M. Lee, S. Peng, T. Guo, P. Chen and T. Wen, *Adv. Mater.*, 2013, **25**, 3727–3732.

46 J. Feng, X. Zhu, Z. Yang, X. Zhang, J. Niu, Z. Wang, S. Zuo, S. Priya, S. (Frank) Liu and D. Yang, *Adv. Mater.*, , DOI:10.1002/adma.201801418.

47 K. Huang, Y. Peng, Y. Gao, J. Shi, H. Li, X. Mo, H. Huang, Y. Gao, L. Ding and J. Yang, *Adv. Energy Mater.*, , DOI:10.1002/aenm.201901419.

48 NREL, Interactive Best Research-Cell Efficiency Chart, https://www.nrel.gov/pv/interactive-cell-efficiency, (accessed 6 December 2025).

49 Precedence Research, Solar Cell Market Size, Share, and Trends 2024 to 2034, https://www.precedenceresearch.com/solar-cell-market, (accessed 13 June 2025).

50 Cervicorn Consulting, Perovskite Solar Cell Market Size, Share, Growth, Report 2025 To 2034, https://www.cervicornconsulting.com/perovskite-solar-cell-market, (accessed 14 June 2025).

51 Industry Arc, Flexible Solar Panel Market – By Type, By Application, By Geography, https://www.industryarc.com/Research/flexible-solar-panel-market-research-800522, (accessed 13 June 2025).

52 A. M. Research, Perovskite Solar Cell Market Size, Share, Competitive Landscape and Trend Analysis Report, https://www.alliedmarketresearch.com/perovskite-solar-cell-market-A13745, (accessed 14 June 2025).

53 G. Tang and F. Yan, *Nano Today*, 2021, **39**, 101155.

54 G. Nazir, A. Rehman, J. Gautam, M. Ikram, S. Hussain, S. Aftab, K. Heo, S.-Y. Lee and S.-J. Park, *Adv. Powder Mater.*, 2025, 100304.

55 N. Rolston, A. D. Printz, J. M. Tracy, H. C. Weerasinghe, D. Vak, L. J. Haur, A. Priyadarshi, N. Mathews, D. J. Slotcavage, M. D. McGehee, R. E. Kalan, K. Zielinski, R. L. Grimm, H. Tsai, W. Nie, A. D. Mohite, S. Gholipour, M. Saliba, M. Grätzel and R. H. Dauskardt, *Adv. Energy Mater.*, , DOI:10.1002/aenm.201702116.

56 H. C. Weerasinghe, N. Macadam, J.-E. Kim, L. J. Sutherland, D. Angmo, L. W. T. Ng, A. D. Scully, F. Glenn, R. Chantler, N. L. Chang, M. Dehghanimadvar, L. Shi, A. W. Y. Ho-Baillie, R. Egan, A. S. R. Chesman, M. Gao, J. J. Jasieniak, T. Hasan and D. Vak, *Nat. Commun.*, 2024, **15**, 1656.

57 Y.-S. Lee, A. Raji, E.-K. Noh, J.-H. Yoon, B. Sung, A. Gasonoo, J. Lee, M.-H. Kim, Y. Choi, Y. Shibasaki and

J.-H. Lee, *J. Inf. Disp.*, 2023, **24**, 263–271.

58 F. Guo, S. Qiu, J. Hu, H. Wang, B. Cai, J. Li, X. Yuan, X. Liu, K. Forberich, C. J. Brabec and Y. Mai, *Adv. Sci.*, , DOI:10.1002/advs.201901067.

59 K. Hwang, Y. Jung, Y. Heo, F. H. Scholes, S. E. Watkins, J. Subbiah, D. J. Jones, D. Kim and D. Vak, *Adv. Mater.*, 2015, **27**, 1241–1247.

60 N. K. Pendyala, S. Magdassi and L. Etgar, *Sol. RRL*, , DOI:10.1002/solr.202200988.

61 S. Das, B. Yang, G. Gu, P. C. Joshi, I. N. Ivanov, C. M. Rouleau, T. Aytug, D. B. Geohegan and K. Xiao, *ACS Photonics*, 2015, **2**, 680–686.

62 T. Lei, F. Li, X. Zhu, H. Dong, Z. Niu, S. Ye, W. Zhao, J. Xi, B. Jiao, L. Ding and Z. Wu, *Sol. RRL*, , DOI:10.1002/solr.202000292.

63 X. Hu, Z. Huang, X. Zhou, P. Li, Y. Wang, Z. Huang, M. Su, W. Ren, F. Li, M. Li, Y. Chen and Y. Song, *Adv. Mater.*, , DOI:10.1002/adma.201703236.

64 H. Wang, Z. Huang, S. Xiao, X. Meng, Z. Xing, L. Rao, C. Gong, R. Wu, T. Hu, L. Tan, X. Hu, S. Zhang and Y. Chen, *J. Mater. Chem. A*, 2021, **9**, 5759–5768.

65 X. Li, P. Li, Z. Wu, D. Luo, H.-Y. Yu and Z.-H. Lu, *Mater. Reports Energy*, 2021, **1**, 100001.

66 K. Ravindranath and S. N. Malhotra, *Corros. Sci.*, 1995, **37**, 121–132.

67 J. Pan, D. Thierry and C. Leygraf, *Electrochim. Acta*, 1996, **41**, 1143–1153.

68 K. Znajdek, M. Sibiński, A. Strąkowska and Z. Lisik, *Opto-Electronics Rev.*, 2016, **24**, 20–24.

69 B. T. Feleki, S. Chandrashekar, R. K. M. Bouwer, M. M. Wienk and R. A. J. Janssen, *Sol. RRL*, 2020, **4**, 2000385.

70 Z. Wu, P. Li, Y. Zhang and Z. Zheng, *Small Methods*, , DOI:10.1002/smtd.201800031.

71 M. Kaltenbrunner, G. Adam, E. D. Głowacki, M. Drack, R. Schwödiauer, L. Leonat, D. H. Apaydin, H. Groiss, M. C. Scharber, M. S. White, N. S. Sariciftci and S. Bauer, *Nat. Mater.*, 2015, **14**, 1032–1039.

72 T. Jin, W. Li, Y. Li, Y. Luo, Y. Shen, L. Cheng and J. Tang, *Adv. Opt. Mater.*, 2018, **6**, 1801153.

73 J. Liu, T. Ye, D. Yu, S. (Frank) Liu and D. Yang, *Angew. Chemie Int. Ed.*, , DOI:10.1002/anie.202307225.

74 J. Li, G. Han, K. Vergeer, H. A. Dewi, H. Wang, S. Mhaisalkar, A. Bruno and N. Mathews, *ACS Appl. Energy Mater.*, 2020, **3**, 777–784.

75 X. Liu, L. Hu, R. Wang, J. Li, H. Gu, S. Liu, Y. Zhou and G. Tu, *Polymers (Basel).*, 2019, **11**, 427.

76 S. Mishra, S. Ghosh and T. Singh, *ChemSusChem*, 2021, **14**, 512–538.

77 Z. Fan, A. Zanelli, C. Monticelli and Q. Li, in *Lightweight Energy: Membrane Architecture Exploiting Natural Renewable Resources*, eds. A. Zanelli, C. Monticelli, N. Jakica and Z. Fan, 2023, pp. 93–149.

78 B. Abdollahi Nejand, P. Nazari, S. Gharibzadeh, V. Ahmadi and A. Moshaii, *Chem. Commun.*, 2017, **53**, 747–750.

79 J. Chen and S. Zhang, *Handbook of Perovskite Solar Cells*, CRC Press, Boca Raton, 2nd edn., 2024.

80 Y. Hu, T. Niu, Y. Liu, Y. Zhou, Y. Xia, C. Ran, Z. Wu, L. Song, P. Müller-Buschbaum, Y. Chen and W. Huang, *ACS Energy Lett.*, 2021, **6**, 2917–2943.

81 H. Wang, Y. Zhao, Z. Wang, Y. Liu, Z. Zhao, G. Xu, T.-H. Han, J.-W. Lee, C. Chen, D. Bao, Y. Huang, Y. Duan and Y. Yang, *Nano Energy*, 2020, **69**, 104375.

82 R. Wang, H. Yu, M. Dirican, L. Chen, D. Fang, Y. Tian, C. Yan, J. Xie, D. Jia, H. Liu, J. Wang, F. Tang, A. M. Asiri, X. Zhang and J. Tao, *ACS Appl. Energy Mater.*, 2020, **3**, 785–793.

83 Z. Lu, Y. Lou, P. Ma, K. Zhu, S. Cong, C. Wang, X. Su and G. Zou, *Sol. RRL*, , DOI:10.1002/solr.202000320.

84 Y. Xie, K. Zhao, H. Wang, Y. Qi, P. Wei and J. Cheng, *ACS Appl. Energy Mater.*, 2023, **6**, 7377–7386.

85 B. Dou, E. M. Miller, J. A. Christians, E. M. Sanehira, T.

View Article Online
DOI: 10.1039/D5YA00363F

R. Klein, F. S. Barnes, S. E. Shaheen, S. M. Garner, S. Ghosh, A. Mallick, D. Basak and M. F. A. M. van Hest, *J. Phys. Chem. Lett.*, 2017, **8**, 4960–4966.

86 H.-H. Chen, J.-Y. Hung and C.-L. Wang, *Chem. Eng. J.*, 2025, **505**, 159508.

87 Y. Yin, Y. Zhou, S. Fu, X. Zuo, Y. Lin, L. Wang, Y. Xue, Y. Zhang, E. H. R. Tsai, S. Hwang, K. Kissenger, M. Li, M. Cotlet, T. Li, K. G. Yager, C. Nam and M. H. Rafailovich, *Small*, , DOI:10.1002/smll.202207092.

88 C.-C. Wu, *RSC Adv.*, 2018, **8**, 11862–11870.

89 A. Seyhan and E. Kartal, *Coatings*, 2023, **13**, 1719.

90 C. Guillén and J. Herrero, *Appl. Surf. Sci.*, 2013, **282**, 923–929.

91 E. I. Bancu, V. Ion, S. Antohe and N. D. Scarisoreanu, *Crystals*, 2025, **15**, 670.

92 P. Ko, T. H. Nhu Tran, L. T. Trinh, J. Y. Seok, S. Kwon, J. Jo, K. Woo and H. Youn, *ACS Appl. Nano Mater.*, 2022, **5**, 12778–12786.

93 P. Garshasbi, N. Alikarami, F. Layaei Vahed, M. Tavakoli Dare, A. Jafari and V. Fakhri, *Surfaces and Interfaces*, 2026, **80**, 108245.

94 H. Bourahla, S. Fernández, Y. K. Ryu, A. Velasco, C. Malkia, A. Boscá, M. B. Gómez-Mancebo, F. Calle and J. Martinez, *Micromachines*, 2025, **16**, 204.

95 A. E. Adetayo, T. N. Ahmed, A. Zakhidov and G. W. Beall, *Adv. Opt. Mater.*, , DOI:10.1002/adom.202002102.

96 K. Sun, P. Li, Y. Xia, J. Chang and J. Ouyang, *ACS Appl. Mater. Interfaces*, 2015, **7**, 15314–15320.

97 J.-H. Kim, H.-J. Seok, H.-J. Seo, T.-Y. Seong, J. H. Heo, S.-H. Lim, K.-J. Ahn and H.-K. Kim, *Nanoscale*, 2018, **10**, 20587–20598.

98 H. Xie, T. Liang, X. Yin, J. Liu, D. Liu, G. Wang, B. Gao and W. Que, *ACS Appl. Energy Mater.*, 2022, **5**, 3081–3091.

99 F. Song, D. Zheng, J. Feng, J. Liu, T. Ye, Z. Li, K. Wang, S. (Frank) Liu and D. Yang, *Adv. Mater.*, , DOI:10.1002/adma.202312041.

100 M. Girtan and B. Negulescu, *Opt. Mater. X*, 2022, **13**, 100122.

101 M. Xie, J. Wang, J. Kang, L. Zhang, X. Sun, K. Han, Q. Luo, J. Lin, L. Shi and C.-Q. Ma, *Flex. Print. Electron.*, 2019, **4**, 034002.

102 E. Dimngaihvungi, M. Singh, B. Pani and A. K. Singh, *Compos. Interfaces*, 2023, **30**, 1449–1481.

103 J. M. C. da Silva Filho, A. D. Gonçalves, F. C. Marques and J. N. de Freitas, *Sol. RRL*, , DOI:10.1002/solr.202100865.

104 M. Najafi, F. Di Giacomo, D. Zhang, S. Shanmugam, A. Senes, W. Verhees, A. Hadipour, Y. Galagan, T. Aernouts, S. Veenstra and R. Andriessen, *Small*, , DOI:10.1002/smll.201702775.

105 Q. Luo, R. Wu, L. Ma, C. Wang, H. Liu, H. Lin, N. Wang, Y. Chen and Z. Guo, *Adv. Funct. Mater.*, , DOI:10.1002/adfm.202004765.

106 N. Ahn, I. Jeon, J. Yoon, E. I. Kauppinen, Y. Matsuo, S. Maruyama and M. Choi, *J. Mater. Chem. A*, 2018, **6**, 1382–1389.

107 Z. Liu, P. You, C. Xie, G. Tang and F. Yan, *Nano Energy*, 2016, **28**, 151–157.

108 E. Jokar, Z. Y. Huang, S. Narra, C. Wang, V. Kattoor, C. Chung and E. W. Diau, *Adv. Energy Mater.*, , DOI:10.1002/aenm.201701640.

109 M. Forouzandeh, M. Heidariramsheh, H. R. Heydarnezhad, H. Nikbakht, M. Stefanelli, L. Vesce and N. Taghavinia, *Carbon N. Y.*, 2024, **229**, 119450.

110 A. Chandrakar and A. Khare, *Sol. Energy*, 2025, **298**, 113649.

111 C. Yang, W. Hu, J. Liu, C. Han, Q. Gao, A. Mei, Y. Zhou, F. Guo and H. Han, *Light Sci. Appl.*, 2024, **13**, 227.

112 A. A. Goje, N. A. Ludin, P. N. A. Fahsyar, U. Syafiq, P. Chelvanathan, A. D. A.-G. Syakirin, M. A. Teridi, M. A. Ibrahim, M. S. Su'ait, S. Sepeai and A. S. H. M. Yasir, *Mater. Renew. Sustain. Energy*, 2024, **13**, 155–179.

View Article Online
DOI: 10.1039/D5YA00363F

113 Y. Rong, Y. Hu, A. Mei, H. Tan, M. I. Saidaminov, S. Il Seok, M. D. McGehee, E. H. Sargent and H. Han, *Science (80-.).*, , DOI:10.1126/science.aat8235.

114 L. A. Castriotta, M. A. Uddin, H. Jiao and J. Huang, *Adv. Mater.*, , DOI:10.1002/adma.202408036.

115 T. D. Raju, V. Murugadoss, K. A. Nirmal, T. D. Dongale, A. V. Kesavan and T. G. Kim, *Adv. Powder Mater.*, 2025, **4**, 100275.

116 Y. Lan, Y. Wang, Y. Lai, Z. Cai, M. Tao, Y. Wang, M. Li, X. Dong and Y. Song, *Nano Energy*, , DOI:10.1016/j.nanoen.2022.107523.

117 S. W. Sharshir, A. A. El-Naggar, H. A. Ismail, M. M. Sami, L. A. Lotfy, M. R. Sharaby, H. Zhao, S.-H. Jang, A. A. Alsakran, N. S. A. EL-Gawaad, M. Ismail, E. Abdelnasser, A. El-Shaer and M. Rashad, *Sol. Energy*, 2025, **299**, 113707.

118 S.-W. Lee, S. Kim, S. Bae, K. Cho, T. Chung, L. E. Mundt, S. Lee, S. Park, H. Park, M. C. Schubert, S. W. Glunz, Y. Ko, Y. Jun, Y. Kang, H.-S. Lee and D. Kim, *Sci. Rep.*, 2016, **6**, 38150.

119 X. Lang, Z. Gao, Y. Zhao, Y. Jiang, X. Liu, M. Li, Y. Gou, C. Chen, D. Zhao, C. Wang, X. Han, J. Ye and C. Xiao, *ACS Appl. Energy Mater.*, 2024, **7**, 11670–11677.

120 N. J. Jeon, J. H. Noh, W. S. Yang, Y. C. Kim, S. Ryu, J. Seo and S. Il Seok, *Nature*, 2015, **517**, 476–480.

121 Y. Xu, Z. Lin, W. Wei, Y. Hao, S. Liu, J. Ouyang and J. Chang, *Nano-Micro Lett.*, 2022, **14**, 117.

122 M. Xu, J. Feng, Z.-J. Fan, X.-L. Ou, Z.-Y. Zhang, H.-Y. Wang and H.-B. Sun, *Sol. Energy Mater. Sol. Cells*, 2017, **169**, 8–12.

123 M. Zhang, Z. Li, Z. Gong, Z. Li and C. Zhang, *Energy Adv.*, 2023, **2**, 355–364.

124 K. Shono, Y. Yamaguchi, U. Perwez, T. Ma, Y. Dai and Y. Shimoda, *Sol. Energy*, 2023, **253**, 137–153.

125 Y. Zhao, S. Wang, H. Ran, Y. Zhang and Y. Tang, *J. Alloys Compd.*, 2023, **965**, 171317.

126 H. Wang and X. Li, *Adv. Mater. Technol.*, , DOI:10.1002/admt.202401606.

127 B. Du, K. He, H. Huang, W. Gao and C. Ran, *Sol. RRL*, , DOI:10.1002/solr.202300620.

128 Z. Yang, Y. Jiang, D. Xu, Z. Wang, X. Gao, X. Lu, G. Zhou, J.-M. Liu and J. Gao, *J. Mater. Chem. A*, 2022, **10**, 22445–22452.

129 V.-D. Tran, S. V. N. Pammi, B.-J. Park, Y. Han, C. Jeon and S.-G. Yoon, *Nano Energy*, 2019, **65**, 104018.

130 W. Li, H. Zhang, S. Shi, J. Xu, X. Qin, Q. He, K. Yang, W. Dai, G. Liu, Q. Zhou, H. Yu, S. R. P. Silva and M. Fahlman, *J. Mater. Chem. C*, 2020, **8**, 4636–4674.

131 J. Qi, H. Xiong, C. Hou, Q. Zhang, Y. Li and H. Wang, *Nanoscale*, 2020, **12**, 3646–3656.

132 Z. Li, C. Jia, Z. Wan, J. Cao, J. Shi, J. Xue, X. Liu, H. Wu, C. Xiao, C. Li, M. Li, C. Zhang and Z. Li, *Nat. Commun.*, 2025, **16**, 1771.

133 S. L. Hamukwaya, H. Hao, Z. Zhao, J. Dong, T. Zhong, J. Xing, L. Hao and M. M. Mashingaidze, *Coatings*, 2022, **12**, 252.

134 N. K. Rana, D. P. Singh and N. Chander, *ACS Appl. Electron. Mater.*, 2024, **6**, 3325–3336.

135 C. Zhang and N.-G. Park, *Commun. Mater.*, 2024, **5**, 194.

136 J. F. Benitez-Rodriguez, D. Chen, M. Gao and R. A. Caruso, *Sol. RRL*, , DOI:10.1002/solr.202100341.

137 J. T. Matondo, H. Hu, Y. Ding, M. Mateen, G. Cheng and J. Ding, *Adv. Mater. Technol.*, , DOI:10.1002/admt.202302082.

138 T. R. Rana, M. Abbas, E. Schwartz, F. Jiang, M. Y. Yaman, Z. Xu, D. S. Ginger and D. MacKenzie, *ACS Energy Lett.*, 2024, **9**, 1888–1894.

139 A. S. Subbiah, S. Mannar, V. Hnapovskyi, A. R. Pininti, B. Vishal, L. V. Torres Merino, O. Matiash, O. Karalis, H. Hempel, A. Prasetio, B. Yildirim, P. Dally, D. Rosas Villalva, M. Babics, L. Xu, A. Razzaq, R. Azmi, F. Xu, H. L. Bristow, E. Ugur, A. Ur Rehman, H. Pasanen, E. Aydin, T. Allen, D. Baran, T. Unold, F. Laquai and S.

View Article Online
DOI: 10.1039/D5YA00363F

De Wolf, *Joule*, 2025, **9**, 101767.

140 I. Susic, A. Kama, L. Gil-Escrig, C. Dreessen, F. Palazon, D. Cahen, M. Sessolo and H. J. Bolink, *Adv. Mater. Interfaces*, , DOI:10.1002/admi.202202271.

141 A. Tara, V. Schröder, A. Paul, N. Maticiuc, M. F. Vasquez-Montoya, J. Dagar, S. Sharma, R. Gupta, E. J. W. List-Kratochvil, E. L. Unger and F. Mathies, *ACS Appl. Mater. Interfaces*, 2024, **16**, 63520–63527.

142 N.-K. Pendyala, A. Kolay, Y. N. Ponnada, A. Guerrero and L. Etgar, *Sustain. Energy Fuels*, 2025, **9**, 1633–1655.

143 R. Swartwout, M. T. Hoerantner and V. Bulović, *ENERGY Environ. Mater.*, 2019, **2**, 119–145.

144 F. U. Kosasih, E. Erdenebileg, N. Mathews, S. G. Mhaisalkar and A. Bruno, *Joule*, 2022, **6**, 2692–2734.

145 S. Wang, L. Tan, J. Zhou, M. Li, X. Zhao, H. Li, W. Tress, L. Ding, M. Graetzel and C. Yi (易陈谊), *Joule*, 2022, **6**, 1344–1356.

146 F. Meng, L. Cheng, F. Wang, K. Chen, Z. Sun and G. Wang, *Adv. Sustain. Syst.*, , DOI:10.1002/adsu.202400695.

147 H. J. Kim, Y. J. Kim, G. S. Han and H. S. Jung, *Sol. RRL*, , DOI:10.1002/solr.202300910.

148 Y. Galagan, F. Di Giacomo, H. Gorter, G. Kirchner, I. de Vries, R. Andriessen and P. Groen, *Adv. Energy Mater.*, , DOI:10.1002/aenm.201801935.

149 G. Burwell, S. Zeiske, P. Caprioglio, O. J. Sandberg, A. M. Kay, M. D. Farrar, Y. R. Kim, H. J. Snaith, P. Meredith and A. Armin, *Sol. RRL*, , DOI:10.1002/solr.202400180.

150 D. Chen, G. Zou, Y. Wu, B. Tang, A. L. Rogach and H. Yip, *Adv. Mater.*, , DOI:10.1002/adma.202414745.

151 H. K. H. Lee, J. Barbé, S. M. P. Meroni, T. Du, C. Lin, A. Pockett, J. Troughton, S. M. Jain, F. De Rossi, J. Baker, M. J. Carnie, M. A. McLachlan, T. M. Watson, J. R. Durrant and W. C. Tsoi, *Sol. RRL*, , DOI:10.1002/solr.201800207.

152 D. I. Kutsarov, E. Rezaee, J. Lambert, W. T. Stroud, A. Panagiotopoulos and S. R. P. Silva, *Adv. Mater. Technol.*, , DOI:10.1002/admt.202401834.

153 S. Castro-Hermosa, G. Lucarelli, M. Top, M. Fahland, J. Fahlteich and T. M. Brown, *Cell Reports Phys. Sci.*, 2020, **1**, 100045.

154 J. Panidi, D. G. Georgiadou, T. Schoetz and T. Prodromakis, *Adv. Funct. Mater.*, , DOI:10.1002/adfm.202200694.

155 X. Jiang, S. Qin, L. Meng, G. He, J. Zhang, Y. Wang, Y. Zhu, T. Zou, Y. Gong, Z. Chen, G. Sun, M. Liu, X. Li, F. Lang and Y. Li, *Nature*, 2024, **635**, 860–866.

156 M. Jahandar, S. Kim and D. C. Lim, *ChemSusChem*, 2021, **14**, 3449–3474.

157 H. Zhang, Y. Luo, T. A. Dela Peña, R. Ma, H. Yan, M. Li, M. Suryawanshi, J. Wu and A. Uddin, *Adv. Mater. Interfaces*, , DOI:10.1002/admi.202500204.

158 F. Liu, K. Liu, S. Rafique, Z. Xu, W. Niu, X. Li, Y. Wang, L. Deng, J. Wang, X. Yue, T. Li, J. Wang, P. Ayala, C. Cong, Y. Qin, A. Yu, N. Chi and Y. Zhan, *Adv. Sci.*, , DOI:10.1002/advs.202205879.

159 L. Kong, Y. Luo, Q. Wu, X. Xiao, Y. Wang, G. Chen, J. Zhang, K. Wang, W. C. H. Choy, Y.-B. Zhao, H. Li, T. Chiba, J. Kido and X. Yang, *Light Sci. Appl.*, 2024, **13**, 138.

160 D. Müller, E. Jiang, P. Rivas-Lazaro, C. Baretzky, G. Loukeris, S. Bogati, S. Paetel, S. J. C. Irvine, O. Oklobia, S. Jones, D. Lamb, A. Richter, G. Siefer, D. Lackner, H. Helmers, C. Teixeira, D. Forgács, M. Freitag, D. Bradford, Z. Shen, B. Zimmermann and U. Würfel, *ACS Appl. Energy Mater.*, 2023, **6**, 10404–10414.

161 D. Dou, H. Sun, C. Li, S. Gan and L. Li, *Adv. Funct. Mater.*, , DOI:10.1002/adfm.202314398.

162 M. Jošt, E. Köhnen, A. Al-Ashouri, T. Bertram, Š. Tomšič, A. Magomedov, E. Kasparavicius, T. Kodalle, B. Lipovšek, V. Getautis, R. Schlatmann, C. A.

View Article Online
DOI: 10.1039/D5YA00363F

Kaufmann, S. Albrecht and M. Topič, *ACS Energy Lett.*, 2022, **7**, 1298–1307.

163 C. Zhang, M. Chen, F. Fu, H. Zhu, T. Feurer, W. Tian, C. Zhu, K. Zhou, S. Jin, S. M. Zakeeruddin, A. N. Tiwari, N. P. Padture, M. Grätzel and Y. Shi, *Energy Environ. Sci.*, 2022, **15**, 1536–1544.

164 G. M. Meheretu, A. K. Worku, M. T. Yihunie, R. K. Koech and G. A. Wubetu, *Heliyon*, 2024, **10**, e36710.

165 M. Yang, H. Wang, W. Cai and Z. Zang, *Adv. Opt. Mater.*, , DOI:10.1002/adom.202301052.

166 J. Mei and F. Yan, *Adv. Mater.*, , DOI:10.1002/adma.202418622.

167 M. Karimipour, S. Khazraei, B. J. Kim, G. Boschloo and E. M. J. Johansson, *Nano Energy*, 2022, **95**, 107044.

168 S. S. Dipta, M. A. Rahim and A. Uddin, *Appl. Phys. Rev.*, , DOI:10.1063/5.0197154.

169 F. Liang, E. Akman, S. Aftab, M. K. A. Mohammed, H. H. Hegazy, X. Zhang and F. Zhang, *InfoMat*, , DOI:10.1002/inf2.12628.

170 M. Ma, W. Bi, Y. Chu, J. Lv, Y. Po-Chuan, Z. Zhang, L. Hong, P. Mao and Y. Zhong, *Adv. Funct. Mater.*, , DOI:10.1002/adfm.202419067.

171 J. Liu, D. Zheng, K. Wang, Z. Li, S. Liu, L. Peng and D. Yang, *Joule*, 2024, **8**, 944–969.

172 T.-Y. Yang, Y. Y. Kim and J. Seo, *APL Mater.*, , DOI:10.1063/5.0064073.

173 S. A. Hashemi, S. Ramakrishna and A. G. Aberle, *Energy Environ. Sci.*, 2020, **13**, 685–743.

174 C. Zhang, L. K. Ono and Y. Qi, *Adv. Funct. Mater.*, , DOI:10.1002/adfm.202314762.

175 H. S. Jung, G. S. Han, N.-G. Park and M. J. Ko, *Joule*, 2019, **3**, 1850–1880.

176 G. G. Jeon, S. E. Yoon, J. Han, H. W. Chun, S. J. Shin, M. J. Choi, S. U. Park, S.-J. Ko, S. Huang, N. Park, J. H. Kim and J. Kim, *Chem. Eng. J.*, 2025, **519**, 164991.

177 L. Wang, D. Zheng, Z. Li, B. Farhadi, L. Peng, S. Zhao, Z. Chang, L. Duan, Y. Cao, H. Wang, Y. Tong, M. Du, K. Wang and S. (Frank) Liu, *Matter*, 2023, **6**, 2987–3005.

178 P. Dąbczyński, M. M. Marzec, Ł. Pięta, K. Fijałkowski, J. Raczkowska, A. Bernasik, A. Budkowski and J. Rysz, *ACS Omega*, 2018, **3**, 3631–3639.

179 W. Fu, A. I. A. Soliman, Y. Zheng, Y. Zhou, Y. Zhang, S. Shan and H. Chen, *Rev. Mater. Res.*, 2025, **1**, 100017.

180 X. Yu, X. Sun, Z. Zhu and Z. Li, *Angew. Chemie Int. Ed.*, , DOI:10.1002/anie.202419608.

181 P. Kumar, M. Eriksson, D. S. Kharytonau, S. You, M. M. Natile and A. Vomiero, *ACS Appl. Energy Mater.*, 2024, **7**, 1421–1432.

182 S. H. Kim, W. I. Choi, K. H. Kim, D. J. Yang, S. Heo and D.-J. Yun, *Sci. Rep.*, 2016, **6**, 33074.

183 M. Althumayri, R. Das, R. Banavath, L. Beker, A. M. Achim and H. Ceylan Koydemir, *Adv. Sci.*, , DOI:10.1002/advs.202405099.

184 E. Kobayashi, R. Tsuji, D. Martineau, A. Hinsch and S. Ito, *Cell Reports Phys. Sci.*, 2021, **2**, 100648.

185 W. Yang, Y. Zhang, C. Xiao, J. Yang and T. Shi, *Nano Mater. Sci.*, , DOI:10.1016/j.nanoms.2025.02.005.

186 W. J. Lee, T.-Y. Cho, S.-H. Choa and S.-K. Cho, *Thin Solid Films*, 2021, **720**, 138524.

187 X. Sun, L. Chen and W. Feng, *Materials (Basel).*, 2024, **17**, 6007.

188 C.-H. Lee, K. S. Yoo, D. Kim, J.-M. Kim and J.-S. Park, *Chem. Eng. J.*, 2025, **503**, 158424.

189 Y. Li, K. Cao, Y. fei Xiong, H. Yang, Y. Zhang, Y. Lin, B. Zhou, J. Huang and R. Chen, *Adv. Mater. Interfaces*, , DOI:10.1002/admi.202000237.

190 D. Kim, H. Lim, S. H. Kim, K. N. Lee, J. You, D. Y. Ryu and J. Kim, *J. Mater. Chem. A*, 2024, **12**, 7452–7469.

191 M. U. Ali, H. Mo, Y. Li and A. B. Djurišić, *APL Energy*, , DOI:10.1063/5.0155845.

192 Y. Weng, G. Chen, X. Zhou, Y. Zhang, Q. Yan and T. Guo, *ACS Appl. Polym. Mater.*, 2023, **5**, 10148–10157.

193 H.-Q. Wang, S. Wang, L. Chen, Z. Yin, S. Mei, Y.

View Article Online
DOI: 10.1039/D5YA00363F

Zhong, Y. Yao, N. Li, J. Wang and W. Song, *Sol. Energy Mater. Sol. Cells*, 2021, **230**, 111278.

194 K. T. Tanko, M. Karimipour, R. Kieftenburg, A. Alcalá-Ibarra and M. Lira-Cantú, *APL Energy*, , DOI:10.1063/5.0270601.

195 R. Cheacharoen, C. C. Boyd, G. F. Burkhard, T. Leijtens, J. A. Raiford, K. A. Bush, S. F. Bent and M. D. McGehee, *Sustain. Energy Fuels*, 2018, **2**, 2398–2406.

196 J. Kim, S. Kim, N. Lee, H. Cho, S. J. Park, J. Kim, N. Lee, S. Kim, S. H. Cho and S. Lee, *Small*, , DOI:10.1002/smll.202501374.

197 M. Cao, W. Ji, C. Chao, J. Li, F. Dai and X. Fan, *Polymers (Basel).*, 2023, **15**, 3911.

198 N. Ahn and M. Choi, *Adv. Sci.*, , DOI:10.1002/advs.202306110.

199 J. Le Bihan, T. Lapi and J. Halloy, *Phys. Soc.*, , DOI:10.48550/arXiv.2502.04205.

200 Q. Tu, D. Kim, M. Shyikh and M. G. Kanatzidis, *Matter*, 2021, **4**, 2765–2809.

201 Z. Li, T. R. Klein, D. H. Kim, M. Yang, J. J. Berry, M. F. A. M. van Hest and K. Zhu, *Nat. Rev. Mater.*, 2018, **3**, 18017.

202 M. Saliba, S. Orlandi, T. Matsui, S. Aghazada, M. Cavazzini, J.-P. Correa-Baena, P. Gao, R. Scopelliti, E. Mosconi, K.-H. Dahmen, F. De Angelis, A. Abate, A. Hagfeldt, G. Pozzi, M. Graetzel and M. K. Nazeeruddin, *Nat. Energy*, 2016, **1**, 15017.

203 J. Yoon, U. Kim, Y. Yoo, J. Byeon, S. Lee, J. Nam, K. Kim, Q. Zhang, E. I. Kauppinen, S. Maruyama, P. Lee and I. Jeon, *Adv. Sci.*, 2021, **8**, 2004092.

204 S. Subba, P. Rai and S. Chatterjee, *Adv. Theory Simulations*, , DOI:10.1002/adts.202400652.

205 N. K. Bansal, S. Mishra, H. Dixit, S. Porwal, P. Singh and T. Singh, *Energy Technol.*, , DOI:10.1002/ente.202300735.

206 Q. Tao, P. Xu, M. Li and W. Lu, *npj Comput. Mater.*, 2021, **7**, 23.

207 C. Jiang, H. He, H. Guo, X. Zhang, Q. Han, Y. Weng, X. Fu, Y. Zhu, N. Yan, X. Tu and Y. Sun, *Nat. Commun.*, 2024, **15**, 6301.

208 P. Baraneedharan, S. Sekar, S. Murugesan, D. Ahamada, S. A. B. Mohamed, Y. Lee and S. Lee, *Nanomaterials*, 2024, **14**, 1867.

209 B. Sandalow, Advance in Perovskite Solar Cells Improves Efficiency, Durability, https://www.mccormick.northwestern.edu/news/articles/2025/01/advance-in-perovskite-solar-cells-improves-efficiency-durability/, (accessed 12 June 2025).

210 US11764001B2, 2023, 1–10.

211 C. Booten, P. Rao, V. Rapp, R. Jackson and R. Prasher, *Joule*, 2021, **5**, 24–46.

212 E. McCalmont, A. Ravilla, T. O'Hara, B. Carlson, J. Kellar and I. Celik, *MRS Adv.*, 2023, **8**, 317–322.

213 E. Leccisi and V. Fthenakis, *Prog. Photovoltaics Res. Appl.*, 2021, **29**, 1078–1092.

214 B. Martin, D. Amos, E. Brehob, M. F. A. M. van Hest and T. Druffel, *Appl. Energy*, 2022, **307**, 118200.

215 A. Tabibi, Solar Energy's Role in Achieving the UN Sustainable Development Goals, https://green.org/2024/01/30/solar-energys-role-in-achieving-the-un-sustainable-development-goals/, (accessed 12 June 2025).

216 J. Gong, S. B. Darling and F. You, *Energy Environ. Sci.*, 2015, **8**, 1953–1968.

217 H. Zhang and N.-G. Park, *DeCarbon*, 2024, **3**, 100025.

218 J. Zhu, J. Xia, Y. Li and Y. Li, *ACS Appl. Mater. Interfaces*, 2025, **17**, 5595–5608.

219 M. Al Atem and Y. Makableh, *Eng*, 2025, **6**, 38.

220 L. A. Castriotta, F. De Rossi and M. Bonomo, *ACS Energy Lett.*, 2025, **10**, 283–286.

221 R. Sharif, A. Khalid, S. W. Ahmad, A. Rehman, H. G. Qutab, H. H. Akhtar, K. Mahmood, S. Afzal and F. Saleem, *Nanoscale Adv.*, 2023, **5**, 3803–3833.

View Article Online
DOI: 10.1039/D5YA00363F

222 J. Berry, Perovskite Solar Cells, https://www.nrel.gov/pv/perovskite-solar-cells, (accessed 12 June 2025).

223 O. PV and U. of Oxford, Oxford PV and Trinasolar announce a landmark Perovskite PV patent licensing agreement, https://www.oxfordpv.com/news/oxford-pv-and-trinasolar-announce-landmark-perovskite-pv-patent-licensing-agreement, (accessed 12 June 2025).

224 Y. Gao, B. Jumayi, P. Wei, C. Song, S. Wang and X. Shen, *Crystals*, 2025, **16**, 24.

225 H. Khir, A. K. Pandey, R. Saidur, M. S. Ahmad and M. Samykano, *J. Power Sources*, 2025, **656**, 238025.

226 D. Liu, T. Zhu, G. Li, Z. Song, Y. Yan and C. Li, *Adv. Energy Mater.*, , DOI:10.1002/aenm.202505840.

227 N. Alam, T. K. Tulka and M. M. Hossain, *e-Prime - Adv. Electr. Eng. Electron. Energy*, 2025, **13**, 101093.

228 Z. Liu, Y. Wang, D. Luo, Z. Xie, Z. Liu, Q. Peng, S. (Frank) Liu and Y. Duan, *Adv. Opt. Mater.*, , DOI:10.1002/adom.202501157.

Thiago F. Santos (B.Sc., M.Sc., Textile Engineering) is a researcher specializing in advanced textile materials and nanomaterials (Borophene) at the Federal University of Rio Grande do Norte (UFRN), Brazil, where he is currently pursuing his Ph.D. in Chemical Engineering. He is a member of the GPIMN – Micro and Nanotechnologies Innovation Research Group. His research focuses on functional textiles, composite materials, borophene-based nanomaterials, and textile systems for energy-related and wearable technologies. He has authored numerous scientific publications and actively contributes to interdisciplinary research in smart textiles, advanced materials, and sustainable energy-related technologies.

Caroliny M. Santos (B.Sc., M.Sc., Textile Engineering) is a researcher specializing in natural fibers, nanomaterials (Silk fibroin), and sustainable composite materials at the Federal University of Rio Grande do Norte (UFRN), Brazil, where she is currently pursuing her Ph.D. in Chemical Engineering. She is a member of the GPIMN – Micro and Nanotechnologies Innovation Research Group. Her research focuses on lignocellulosic fibers, polymer composites, nanostructured materials, and advanced textile systems for sustainable engineering applications. She has authored several scientific publications and actively contributes to interdisciplinary research in sustainable materials, functional textiles, and advanced material technologies.

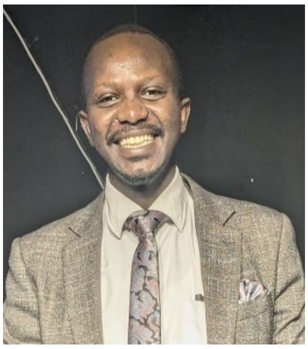

View Article Online
DOI: 10.1039/D5YA00363F

Bahati Shabani Nzeyimana is a Ph.D. Research Scholar at the PG& Research Department of Environmental Sciences at Bishop Heber College (Autonomous), affiliated to Bharathidasan University, India. His research focuses on resource optimization, circular economy, decarbonization, and integrating sustainability in higher education–industry partnerships. He has published in SCIE outlets and contributed to multiple book chapters. He received the best research award at the college level and was recognized as the best reviewer for international journals in sustainability and environmental sciences. His professional experience includes sustainability auditing, ESG advisory services, and applied environmental management for higher education institutions and industry partners.

Dr. Bhargav Akkinepally is a materials scientist specializing in nanomaterials and sustainable energy storage. His research focuses on batteries, supercapacitors, MXenes, solid electrolytes, and advanced electrochemical systems. He has authored several high-impact publications and actively contributes to international conferences and interdisciplinary research in advanced energy materials and electrochemical technologies.

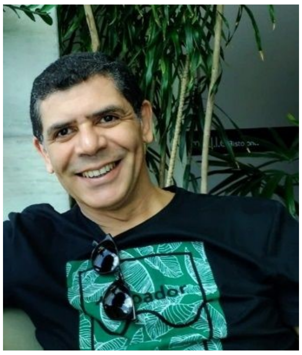

Dr. Domingos F. S. Souza is a Professor of Chemical Engineering at the Federal University of Rio Grande do Norte (UFRN), Brazil, and coordinator of the Laboratory of Alternative Energy and Transport Phenomena (LEAFT). His research focuses on process modeling, simulation, and optimization applied to chemical, biotechnological, and energy systems. His work includes bioenergy, biomass valorization, nanomaterials, microfluidics, and sustainable chemical processes. He actively contributes to interdisciplinary research in energy technologies, biorefineries, and environmental process engineering.

Dr. J. H. O. Nascimento is an Associate Professor and Head of the Textile Engineering Department and leader of the GPIMN - Micro and Nanotechnologies Innovation Research Group at a Brazilian federal university. His research focuses on nanotechnology, graphene-based materials, nanocoatings, nanobiotechnology, and sustainable textile processes. His work explores

View Article Online
DOI: 10.1039/D5YA00363F

advanced functional materials for smart textiles, environmental technologies, photocatalysis, antimicrobial systems, and energy-related applications. He has authored numerous peer-reviewed publications and book chapters and actively contributes to the international scientific community as a reviewer and editor for leading journals.

View Article Online
DOI: 10.1039/D5YA00363F

DATA AVAILABILITY STATEMENT

The datasets created in VOSviewer and analyzed in this study can be obtained from the corresponding author upon reasonable request. Data presented in the figures are subject to specific restrictions to ensure relevance and manageability for targeted analyses.

1) **Figure 4.** a) Historical Trend of Documents and Citations **1972-2024**; and b) Linear Fit and Projections 2012-2030.

   String in Scopus: (“flexible”) AND (“perovskite”)

   Restrictions: language (English), period (1972-2024), or document type (Articles only)

2) **Figure 1.** Thermal map of keyword frequency for f-PeSCs (**a**) in 2012-2018, and (**b**) in 2019-2024; % occurrences of terms (**c**) in 2012-2018, and (**d**) in 2019-2024.

Nº total of occurrences in 2012-2018: 10 occurrences

Nº total of occurrences in 2019-2024: 35 occurrences